Simulated Three-Dimensional Ground-Water Flow in the Lockport Group, A Fractured-Dolomite Aquifer Near Niagara Falls, New York

United States Geological Survey Water-Supply Paper 2487

Prepared in cooperation with the U.S. Environmental Protection Agency

AVAILABILITY OF BOOKS AND MAPS OF THE U.S. GEOLOGICAL SURVEY

Instructions on ordering publications of the U.S. Geological Survey, along with prices of the last offerings, are given in the current-year issues of the monthly catalog "New Publications of the U.S. Geological Survey." Prices of available U.S. Geological Survey publications released prior to the current year are listed in the most recent annual "Price and Availability List." Publications that may be listed in various U.S. Geological Survey catalogs (**see back inside cover**) but not listed in the most recent annual "Price and Availability List" may be no longer available.

Order U.S. Geological Survey publications **by mail** or **over the counter** from the offices given below.

BY MAIL

Books

Professional Papers, Bulletins, Water-Supply Papers, Techniques of Water-Resources Investigations, Circulars, publications of general interest (such as leaflets, pamphlets, booklets), single copies of Preliminary Determination of Epicenters, and some miscellaneous reports, including some of the foregoing series that have gone out of print at the Superintendent of Documents, are obtainable by mail from

U.S. Geological Survey, Information Services
Box 25286, Federal Center, Denver, CO 80225

Subscriptions to Preliminary Determination of Epicenters can be obtained ONLY from the

Superintendent of Documents
Government Printing Office
Washington, DC 20402

(Check or money order must be payable to Superintendent of Documents.)

Maps

For maps, address mail orders to

U.S. Geological Survey, Information Services
Box 25286, Federal Center, Denver, CO 80225

OVER THE COUNTER

Books and Maps

Books and maps of the U.S. Geological Survey are available over the counter at the following U.S. Geological Survey Earth Science Information Centers (ESIC's), all of which are authorized agents of the Superintendent of Documents:

- **ANCHORAGE, Alaska**—Rm. 101, 4230 University Dr.
- **LAKEWOOD, Colorado**—Federal Center, Bldg. 810
- **MENLO PARK, California**—Bldg. 3, Rm. 3128, 345 Middlefield Rd.
- **RESTON, Virginia**—USGS National Center, Rm. 1C402, 12201 Sunrise Valley Dr.
- **SALT LAKE CITY, Utah**—Federal Bldg., Rm. 8105, 125 South State St.
- **SPOKANE, Washington**—U.S. Post Office Bldg., Rm. 135, West 904 Riverside Ave.
- **WASHINGTON, D.C.**—Main Interior Bldg., Rm. 2650, 18th and C Sts., NW.

Maps Only

Maps may be purchased over the counter at the following U.S. Geological Survey office:

- **ROLLA, Missouri**—1400 Independence Rd.

Simulated Three-Dimensional Ground-Water Flow in the Lockport Group, a Fractured-Dolomite Aquifer near Niagara Falls, New York

By **RICHARD M. YAGER**

Prepared in cooperation with the
U.S. Environmental Protection Agency

U.S. GEOLOGICAL SURVEY WATER SUPPLY PAPER 2487

U.S. DEPARTMENT OF THE INTERIOR
BRUCE BABBITT, Secretary

U.S. GEOLOGICAL SURVEY
Robert M. Hirsch, Director

UNITED STATES GOVERNMENT PRINTING OFICE:1996

For sale by the
U.S. Geological Survey
Branch of Information Services
Box 25286
Denver, Co 80225-0286

Library of Congress Cataloging in Publication Data
Yager, Richard M.
Simulated three-dimensional ground-water flow in the Lockport Group, a fractured-dolomite aquifer near Niagara Falls, New York / by Richard M. Yager.
p. cm. – (U.S. Geological Survey water-supply paper ; 2487)
"Prepared in cooperation with the U.S. Environmental Protection Agency."
Includes bibliographical references.
Supt. of Docs. no.: I 19.13:2487
1. Groundwater flow — New York (State) — Niagara Falls Region. 2. Aquifers —New York (State) —Niagara Falls Region. 3. Lockport Group. I. United States. Environmental Protection Agency. II. Title. III. Series.
GB1197.7.y34 1997
551.49´09747–dc21

96–30075
CIP
ISBN 0–607–86219–X

CONTENTS

Figures

TABLES

CONVERSION FACTORS AND VERTICAL DATUM

Multiply	By	To obtain
	Length	
inch (in)	25.4	millimeter
foot (ft)	0.3048	meter
mile (mi)	1.609	kilometer
	Area	
square mile (mi^2)	2.59	square kilometer
	Flow	
gallon per minute (gal/min)	0.06308	liter per second
cubic feet per day (ft^3/d)	0.02832	cubic meter per day
cubic feet per second per square mile [(ft3/s)/mi2]	0.0109	cubic meters per second per square kilometer
	Transmissivity	
foot squared per day (ft^2/d)	0.0929	meter squared per day
	Hydraulic conductivity	
foot per day (ft/d)	0.3048	meter per day
	Pressure	
pounds per square inch (psi)	6.895	kilopascal

Sea level: In this report, "sea level" refers to the National Geodetic Vertical Datum of 1929—a geodetic datum derived from a general adjustment of the first-order level nets of both the United States and Canada, formerly called Sea Level Datum of 1929.

Simulated Three-Dimensional Ground-Water Flow in the Lockport Group, A Fractured Dolomite Aquifer Near Niagara Falls, New York

***By* Richard M. Yager**

Abstract

A three-dimensional model was developed to estimate rates and directions of ground-water flow in the Lockport Group, a fractured bedrock aquifer near Niagara Falls, N.Y. The 10-layer model represents an area of 110 square miles. Water within the Lockport Group flows through the weathered bedrock surface and several underlying horizontal fracture zones at or near stratigraphic contacts; the fracture zones are connected by high-angle fractures and by subcrop areas where they intersect the bedrock surface. The fracture network was assumed to function as a porous medium at the scale of the model. The fracture zones were represented by model layers, and connections between the zones were represented by vertical leakage between the layers.

The Niagara Escarpment and the Niagara River Gorge form natural hydrologic boundaries on the northern and western sides of the modeled area, respectively. No-flow, defined flow, or constant-head boundaries for the southern and eastern sides were selected on the basis of potentiometric-surface features indicated on maps of each layer. The upper boundary was specified as constant head in areas underlying the Niagara River and its tributaries, and as constant flow representing recharge to the weathered bedrock elsewhere. The bottom boundary was specified as no-flow because an overpressured gas reservoir underlies the Lockport Group and prevents vertical flow of water to or from the modeled area. Several manmade hydraulic structures, including a reservoir, tunnels excavated in bedrock, and an extensive drainage system surrounding hydropower conduits, also were represented as boundaries.

Results of steady-state simulations were compared with (1) the measured potentiometric surface of the weathered bedrock zone, (2) average heads measured by piezometers in fracture zones, (3) low-flow measurements of springs and streams, and (4) measurements of discharge from tunnels and excavations. Trial-and-error and nonlinear regression were used to estimate recharge, transmissivity of the weathered bedrock and fracture zones, and vertical hydraulic conductivity of the bedrock. Nonlinear regression enabled identification and estimation of values for model parameters to which the measured heads and flows were sensitive.

Results indicated that (1) measured flow into the Falls Street tunnel—an unlined storm sewer excavated in bedrock—exceeds the amount that can be sustained by the aquifer; therefore, a connection between the tunnel and the Niagara River can be assumed; (2) recharge within the urban parts of the modeled area is greater than in rural areas, possibly because of losses from the municipal water supply or infiltration from unlined storm sewers that intersect the bedrock; and (3) lowlands near the Niagara River might contain widespread areas in which ground water flows upward and is discharged through evapotranspiration and surface drainage.

Alternative concepts of the aquifer system that closely reproduced the measured heads and flows used for calibration were identified through nonlinear regression. The first included additional zones of recharge, the second included different model boundary conditions, and the third included horizontal anisotropy within model layers. The calibrated model and the two best alternative models were used to estimate ground-water flow rates at 21 waste-disposal sites.

INTRODUCTION

The corridor adjacent to the Niagara River from Buffalo to Niagara Falls, N.Y. (fig. 1) is highly industrialized as a result of the abundant water supply for manufacturing and power generation. The disposal of industrial wastes, either through direct discharge to the river or migration from burial sites, has degraded the quality of ground water and surface water within the Niagara River basin, the Niagara River, and Lake Ontario. More than 200 waste-disposal sites have been identified within 3 mi of the Niagara River, and chemical contaminants are likely to have leaked from nearly a third of these sites (Niagara River Toxics Committee, 1984). The primary pathway for contaminant transport from many of the waste-disposal sites to the Niagara River is the Lockport Group[1], the fractured dolomite aquifer that underlies the area.

1. Usage of the New York State Geological Survey; designated "Lockport Dolomite" by the U.S. Geological Survey.

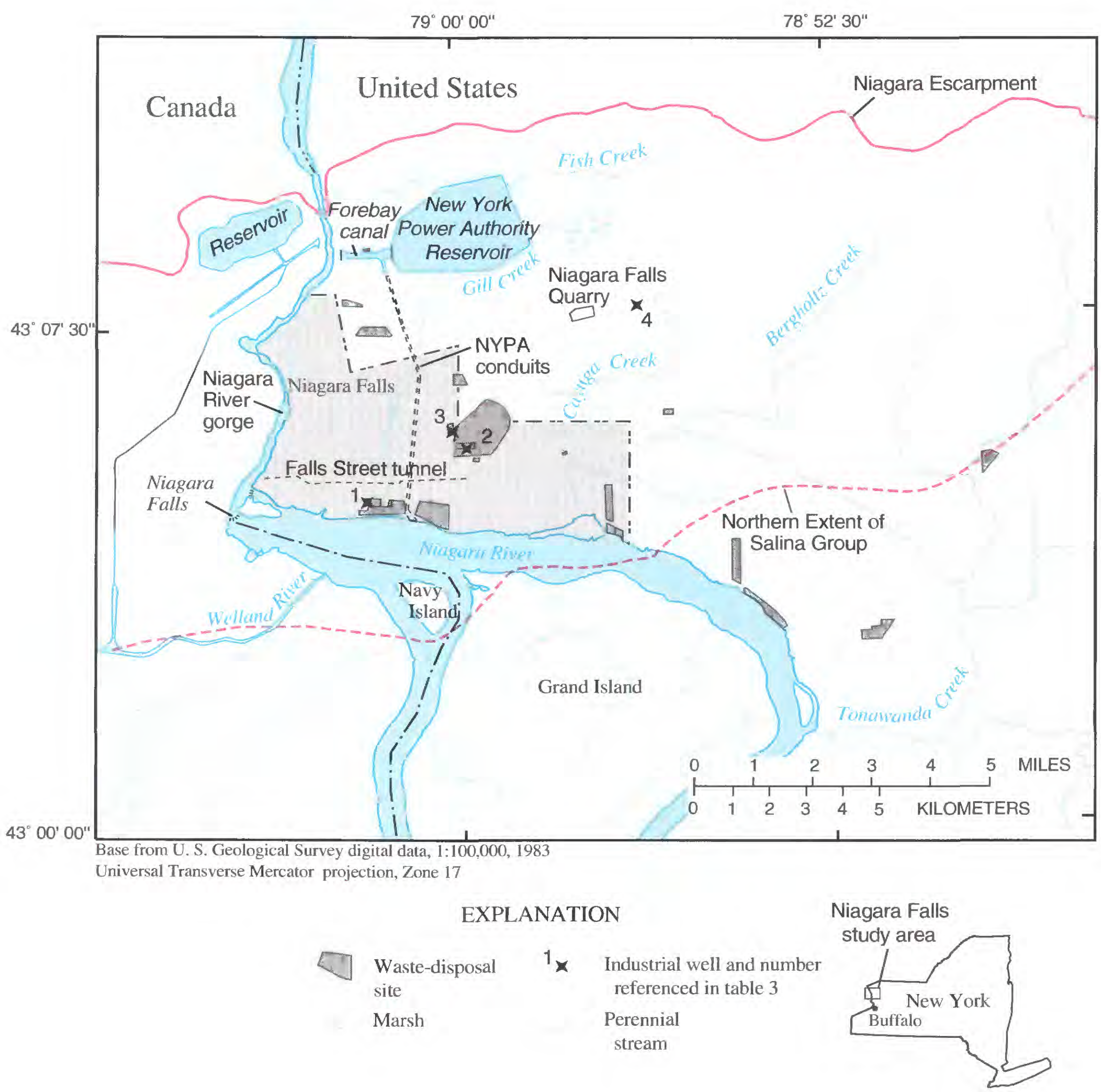

Figure 1. Geographic features of the Niagara Falls area and locations of waste-disposal sites.

In 1986, the USGS (U.S. Geological Survey), in cooperation with the USEPA (U.S. Environmental Protection Agency), began a 5-year study to investigate the regional ground-water-flow system in the Niagara Falls area. Field investigations included (1) drilling 13 boreholes to obtain information on stratigraphy and fracture distribution, (2) installing multilevel piezometers to obtain vertical profiles of hydraulic head, transmissivity, and ground-water chemistry, and (3) pumping water from isolated fracture zones in the bedrock to determine the transmissivity and degree of vertical connection between fracture zones. The resulting information was used to develop a three-dimensional model of ground-water flow through the Lockport Group, and the model was used to delineate the principal recharge and discharge areas and to estimate rates and directions of ground-water flow. Flow rates at 21 waste-disposal sites designated as priority sites by USEPA (C. L. Zafonte, U.S. Environmental Protection Agency, written commun., 1989) were also estimated from model results. Flow rates calculated by the model can be used to specify boundary conditions in smaller models of individual waste-disposal sites within the modeled area by methods described in Buxton and Reilly (1987).

The hydrogeology of the Lockport Group has been described by Johnston (1964), Novakowski and Lapcevic (1988), and Tepper (1989). Models of ground-water flow in the Lockport Group in the Niagara Falls area were developed by M.P. Bergeron (U.S. Geological Survey, written commun., 1984) and Maslia and Johnston (1984); several other models of the Lockport Group were developed for specific site investigations (Mercer and others, 1983; GeoTrans, 1987; Woodward-Clyde Consultants, 1989).

This report describes three-dimensional ground-water flow through the Lockport Group in the Niagara Falls area simulated by a model developed through a parameter-estimation method based on nonlinear regression. The report (1) describes the hydrogeologic setting of the Niagara Falls area, (2) discusses the model design and calibration, (3) describes the calibration by nonlinear regression procedures to estimate model parameter values, (4) presents results of model simulations, including maps showing the general direction and rate of flow through the aquifer and an estimated ground-water budget, and (5) presents estimates of ground-water flow rates beneath selected waste-disposal sites.

HYDROGEOLOGIC SETTING

The Niagara Falls area is underlain by glacial sediments consisting primarily of till and lacustrine silt and clay. The glacial sediments are underlain by carbonate bedrock.

Surficial Material

Reported hydraulic conductivity of the glacial sediments at two sites in Niagara Falls ranges from 9×10^{-1} to 2×10^{-5} ft/d with a median of 2×10^{-3} ft/d (E.C. Jordan Co., 1985; Conestoga-Rovers and Associates and Woodward-Clyde Consultants, 1990). These deposits are assumed to be isotropic, as shown by Desaulniers and others (1981), who compared vertical hydraulic-conductivity values from laboratory tests of core samples with horizontal hydraulic-conductivity values from slug tests in similar deposits in the Niagara Peninsula of Ontario. The thickness of glacial sediments ranges from less than 5 ft near the Niagara Escarpment to more than 80 ft along Tonawanda Creek (fig. 1). These deposits act as a confining unit that limits the flow of water to and from the more permeable weathered bedrock below. Ground-water flow in these deposits is generally downward in recharge areas near topographic highs and upward in discharge areas near streams and in other low-lying areas.

Lockport Group

The glacial sediments are underlain by about 170 ft of virtually undeformed dolomites and limestones of the Lockport Group of the Niagaran Series (Middle Silurian) (table 1). The nomenclature for the Lockport Group given in table 1 has been published in Brett and others (1995). The Lockport Group is in turn underlain by the Clinton Group, which consists of about 100 ft of shale and limestone, and by the Medina Group, which consists of about 110 ft of sandstone and shale. These units strike approximately east-west and dip to the south at about 25 ft/mi in a homoclinal structure. All of the units crop out along the Niagara Escarpment (fig. 1).

Water-Bearing Fractures

The hydraulic properties of the Lockport Group are related primarily to secondary permeability caused by fractures and vugs. These openings have been widened

Table 1. Bedrock stratigraphy of the Niagara Falls area

[Modified from Miller and Kappel, 1987, with additional data from Fisher and Brett, 1981; Brett and Calkin, 1987, Brett and others, 1995.]

System	Series	Group	Formation	Average thickness (feet)	Description
Silurian	Cayugan	Salina	Vernon Shale	57 (in study area)	Green and red shale.
	Niagaran	Lockport	Guelph Dolomite	33	Brownish-gray to dark gray, fine to medium, thick-bedded dolomite, with some argillaceous dolomicrite, particularly near contact with the Vernon Shale.
			Eramosa Dolomite	52	Brownish-gray, biostromal, bituminous, medium- to massive-bedded dolomite, with some argillaceous dolomicrite.
			Goat Island Dolomite	41	Light olive-gray to brownish gray, fine to medium crystalline, thick- to massive-bedded saccharoidal, cherty dolomite, with argillaceous dolomicrite near top of formation.
			Gasport Limestone	33	Basal unit is dolomitic, crinoidal grainstone, overlain by argillaceous limestone.
		Clinton	DeCew Dolomite	10	Very finely crystalline dolomite, medium to dark gray, thin to medium bedded.
			Rochester Shale	60	Dark-gray calcareous shale weathering to light gray to olive
			Irondequoit Limestone	12	Light-gray to pinkish-white coarse-grained limestone.
			Reynales Limestone	10	White to yellowish-gray shaly limestone and dolomite
			Neahga Shale	5	Greenish-gray soft fissile shale.
		Medina[1]	Thorold Sandstone	8	Greenish-gray shaly sandstone
			Grimsby Sandstone	45	Reddish-brown to greenish-gray cross-bedded sandstone interbedded with red to greenish-gray shale.
			Power Glen Shale	40	Gray to greenish-gray shale interbedded with light-gray sandstone.
			Whirlpool Sandstone	20	White, quartzitic sandstone.
Ordovician	Upper	Richmond	Queenston Shale	1,200	Brick-red sandy to argillaceous shale.

[1] Designated Albion Group by the U.S. Geological Survey

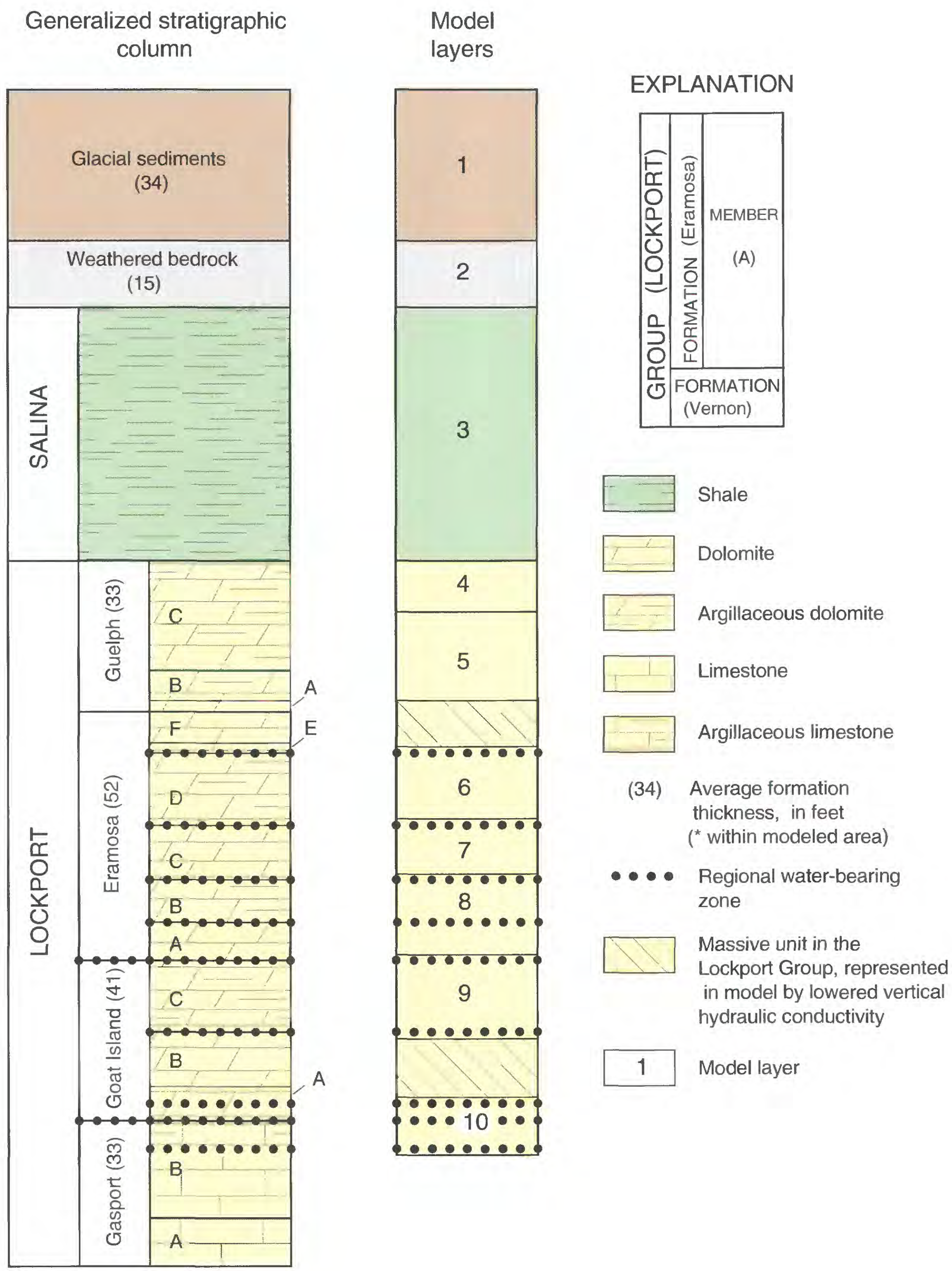

Figure 2. Relations among stratigraphy (from Brett and others, 1995), regional water-bearing zones (from Tepper and others, 1991), and model layers. Use of proposed nomenclature for the Lockport Group does not constitute formal acceptance by the U.S. Geological Survey.

by chemical dissolution in areas where water with a low dissolved-solids concentration circulates through the bedrock. The principal water-bearing zones in the Lockport Group are the weathered bedrock surface and horizontal-fracture zones near stratigraphic contacts (Tepper and others, 1991) (fig. 2). The rock matrix transmits only negligible amounts of ground water because the primary porosity is extremely low.

The weathered bedrock ranges from 10 to 25 ft in thickness and contains many closely spaced horizontal fractures that are connected by high-angle fractures. The fractures in this zone show signs of weathering and have been widened by chemical dissolution. A wide range of horizontal hydraulic-conductivity values for the weathered bedrock have been reported (table 2). Values obtained from slug and constant-head injection tests range from 0.003 to 570 ft/d, and values obtained from aquifer tests range from 0.2 to 200 ft/d. The aquifer tests probably are the more representative because the tests affect a larger volume of the aquifer than slug and constant-head injection tests. The median value of horizontal hydraulic conductivity of the weathered bedrock estimated from seven single-hole aquifer tests conducted during this study was 40 ft/d. The hydraulic conductivity of the weathered bedrock is highest in areas where the bedrock crops out in the Niagara River because river water has widened fractures through dissolution of the rock matrix. The hydraulic conductivity in these areas exceeds 100 ft/d, as indicated by an aquifer test conducted by Legette, Brashears, and Graham, Inc. (1979).

Nine horizontal-fracture zones that extend throughout the study area were delineated through correlation of hydrogeologic information that included (1) fractures identified in drill cores and on acoustic-televiewer and other geophysical logs, (2) hydraulic testing, (3) geochemical analysis, and (4) mapping of seepage zones in outcrops and quarries (Tepper, 1989). The horizontal-fracture zones are as much as 2 ft thick and contain one or more fractures that have developed near lithologic contacts, which are planes of structural weakness within the Lockport Group. These horizontal fractures are probably unloading joints that developed during isostatic rebound, both from erosional unloading and deglaciation (Tepper and others, 1991). The median transmissivity of the horizontal-fracture zones, estimated from slug tests conducted during this study in 19 fracture zones in 7 boreholes was 100 ft^2/d, with a range of 30 to 700 ft^2/d.

The transmissivity of each of the upper six horizontal-fracture zones at depths exceeding 80 ft below bedrock surface is about 2 orders of magnitude lower

Table 2. Hydraulic-conductivity values of weathered bedrock estimated from hydraulic tests

Location	Data source	Hydraulic conductivity (feet per day) Minimum	Maximum
Slug and constant-head injection tests			
Bell Aerospace Textron	Golder and Associates, 1987	0.3	9
Niagara River	Golder and Associates, 1990a	.1	.4
Necco Park landfill	Woodward-Clyde Consultants, 1984	2.2	280
Necco Park landfill	Woodward-Clyde Consultants, 1989	.003	230
DuPont Buffalo Avenue plant	Woodward-Clyde Consultants, 1983	90	570
102nd Street landfill	Conestoga-Rovers and Associates, 1990	.02	280
Stauffer Chemical plant	New York Power Authority, 1986	.03	140
All		.003	570
Aquifer tests			
U.S. Geological Survey	This study	6	180
Occidental Buffalo Avenue plant	Legette, Brashears and Graham, 1979	55	120
Cecos International	Ground Water Associates, 1986	20	160
Carborundum Specialty Products	Ecology and Environment, 1987	100	200
Necco Park landfill	Woodward-Clyde Consultants, 1988	5	30
Reichold-Varcum Chemicals	Conestoga-Rovers and Associates, 1988	.2	2
Bell Aerospace Textron	Golder and Associates, 1990b	5	52
All		1	200

than that at lesser depths. Below the 80-ft depth, the weight of the overlying rock mass has prevented the opening of fractures along the stratigraphic contacts (D.H. Tepper, U.S. Geological Survey, oral commun., 1990). In contrast, the transmissivity of the three horizontal-fracture zones at the base of the Lockport Group, in the Goat Island and Gasport Formations, is relatively unaffected by the weight of the overlying rock mass at depths less than about 150 ft below the bedrock surface. The persistence of fracture openings at greater depths in these zones could be related to the significant erosion that occurred along this contact before burial (D.H. Tepper, U.S. Geological Survey, oral commun., 1992). This erosion surface apparently has enough relief to prevent closure of the open fractures by the weight of the overlying rock mass.

The horizontal-fracture zones in some areas are connected by high-angle fractures, which are probably most common where joints have formed or been enlarged through stress relief along the Niagara River Gorge and near rock excavations (American Falls International Board, 1974). The vertical hydraulic conductivity of the high-angle fractures connecting horizontal-fracture zones was estimated from the results of cross-hole tests conducted near the Niagara Falls quarry (fig. 1) as part of this study (Yager and Hill, 1991). In these tests, the fracture zones that were intersected by the pumped borehole and four observation boreholes were isolated with inflatable packers. One horizontal-fracture zone was pumped, and drawdown in adjacent fracture zones was measured with pressure transducers. The horizontal and vertical hydraulic conductivities of the fracture zones were estimated by numerical simulation of the observed drawdown distribution to be 20 ft/d and 0.3 ft/d, respectively, indicating anisotropy (ratio of horizontal to vertical hydraulic conductivity) of 70:1 (Yager and Hill, 1991). The anisotropy is assumed to be much higher elsewhere in the study area because the cross-hole tests were conducted at a site that overlies a suspected regional fracture zone and could therefore contain a higher density of high-angle fractures than other areas in the region (Yager and Kappel, 1987).

Ground-Water Flow Patterns

The potentiometric-surface delineation of the weathered bedrock (fig. 3A) is based on head measurements in 144 wells completed in weathered bedrock over a 30-year period (1960–90). The potentiometric-surface contours are therefore a composite representation that is assumed to represent average, steady-state conditions. This assumption is supported by a hydrograph recorded in the city of Niagara Falls that shows little change in the mean annual head during 1976–86 (Miller and Kappel, 1987, fig. 4). Heads measured in multilevel piezometers during 1987–92 were used to delineate the potentiometric surface in the underlying fracture zones. The potentiometric surface in the Gasport Limestone at the base of the Lockport Group (fig. 3B) parallels the potentiometric surface in the weathered bedrock but the surface is smoother because it is less affected by land-surface topography and local variability in recharge.

Ground water flows through the Lockport Group from topographic highs near the Niagara Escarpment northward toward the escarpment, and south and westward toward low-lying areas near the Niagara River and outcrop areas along the Niagara River Gorge (fig. 3). Recharge enters the weathered bedrock as infiltration from the overlying glacial sediments and enters the horizontal-fracture zones where they intersect the bedrock surface and high-angle fractures. Recharge also enters the Lockport Group as infiltration from the Niagara River in areas where the bedrock crops out in the river bottom (fig. 3A). Pumping from the Lockport Group by an industrial production well increases the rate of infiltration from the Niagara River near the city of Niagara Falls. Manmade structures increase recharge to the bedrock in other areas: for example, the New York Power Authority (NYPA) reservoir (fig. 3A) is surrounded by a dike that maintains a water level about 40 ft above natural land surface, and leakage from the municipal water supply and unlined storm sewers in the city of Niagara Falls probably contributes recharge to the weathered bedrock.

The Niagara River is the ultimate point of discharge for most ground water in the Niagara Falls area. Discharge from the weathered bedrock to the river and its tributaries generally flows upward through overlying glacial sediments. In a few locations, however, where bedrock is exposed at land surface, ground water discharges directly to stream channels and springs; it also discharges directly to land surface along the Niagara Escarpment and Niagara River Gorge, where the horizontal-fracture zones crop out. Excavations that intersect fracture zones in the bedrock also provide points for ground-water discharge. The largest of these is the Falls Street tunnel (an unlined storm sewer, fig. 1) in which discharge has been estimated to exceed 10^6 ft^3/d (Camp, Dresser, and McKee Environmental

Engineers, 1982). Discharge to the tunnel is greatest where it crosses a drain system surrounding the NYPA conduits, which carry water from intakes at the Niagara River to the forebay canal (a storage reservoir) (fig. 1). The drain system, which extends the length of the conduits, intersects the entire Lockport Group and has an effective transmissivity greater than 10^6 ft^2/d, as calculated from the measured hydraulic gradient and the flow into the Falls Street tunnel. A grout curtain surrounding the intakes prevents direct hydraulic connection between the river and the drain (Miller and Kappel, 1987).

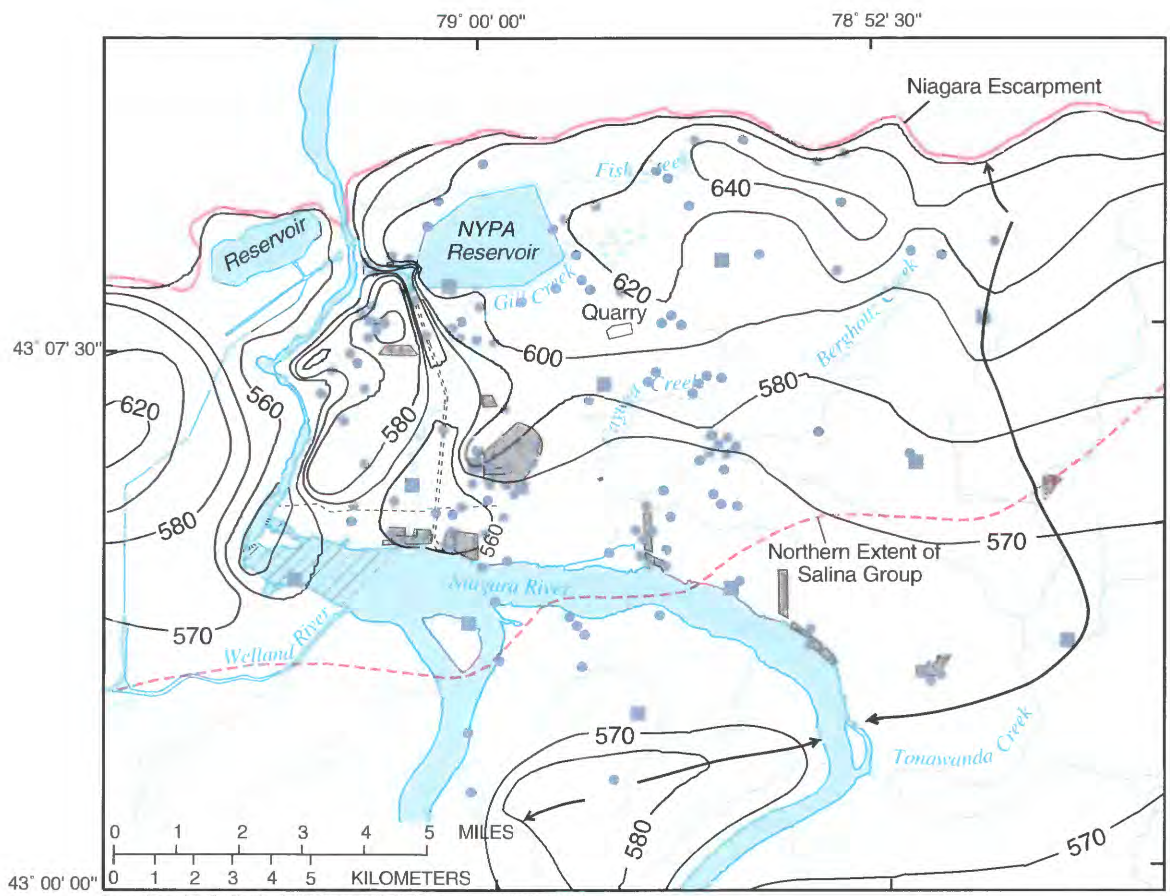

Base from U. S. Geological Survey digital data, 1:100,000, 1983
Universal Transverse Mercator projection, Zone 17

EXPLANATION

- Area where bedrock crops out in river.
- Waste-disposal site
- Perennial stream
- Marsh
- 580 — POTENTIOMETRIC CONTOUR, IN FEET. Shows altitude of hydraulic head measured in selected wells. Contour interval 20 feet except where noted.
- Ground-water flow path that coincides with model boundary
- Well completed in weathered-bedrock
- Multilevel piezometer

Figure 3A. Steady-state potentiometric-surface altitude in weathered bedrock.

Ground-water flow in the Lockport Group is generally horizontal along the plane of the gently dipping horizontal-fracture zones. These zones are confined aquifers separated from each other by the rock matrix, which acts as a confining layer that allows vertical leakage through high-angle fractures. Vertical gradients are downward in recharge areas and in discharge areas near bedrock outcrops along the Niagara River Gorge. Vertical gradients are upward in discharge areas along the Niagara River upstream of Niagara Falls and beneath tributaries

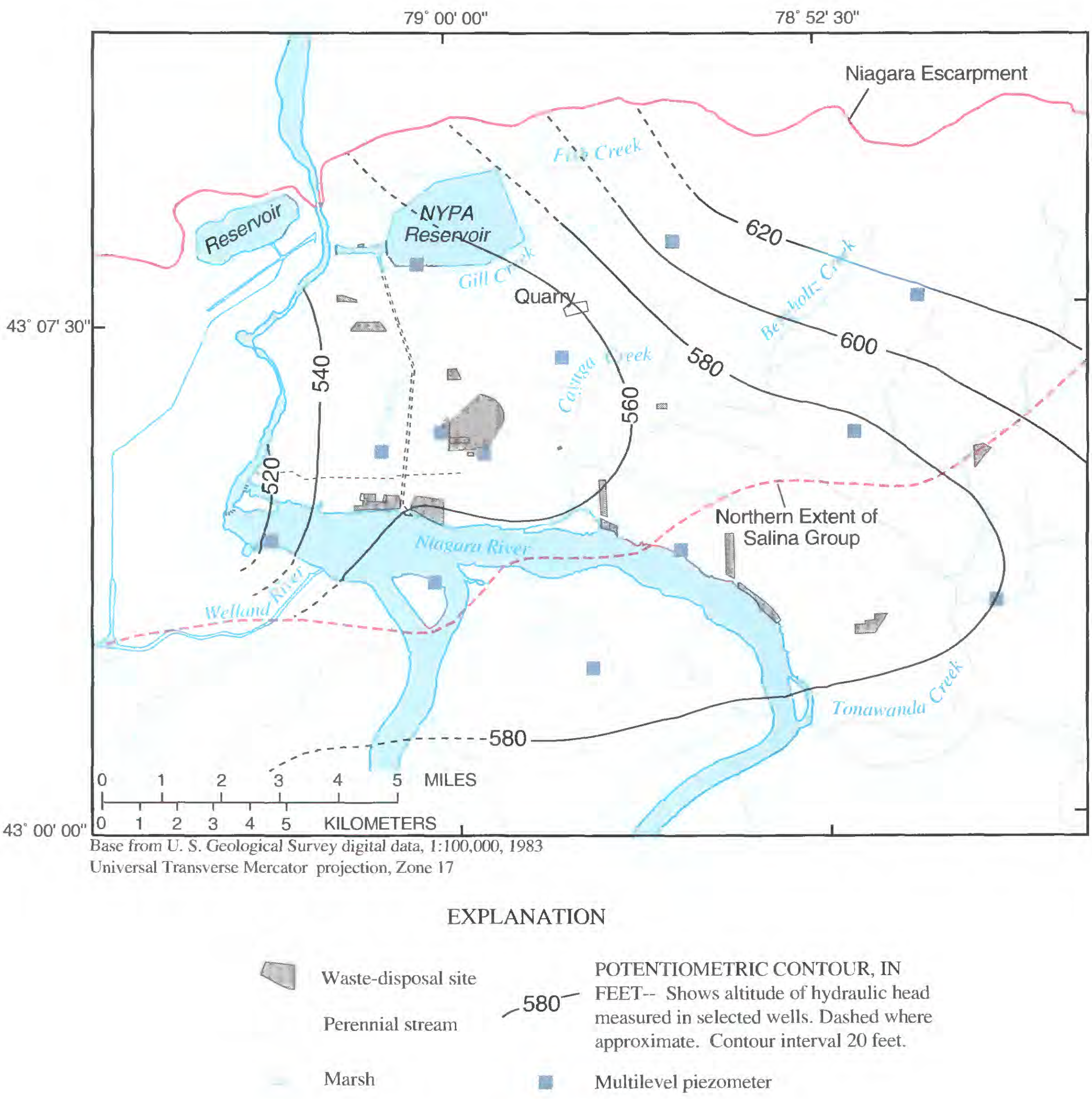

Figure 3B. Steady-state potentiometric-surface altitude in Gasport Limestone at base of Lockport Group.

to the river throughout the study area. The presence of saline water in the lower part of the Lockport Group indicates that present-day circulation of ground water is largely restricted to the shallow flow system. The saline water is a sodium-chloride type water with a dissolved solids (DS) concentration greater than 6,000 mg/L, whereas the water in the upper part of the Lockport Group is a calcium-sulfate type with a DS concentration of less than 3,000 mg/L (Noll, 1986). The freshwater lens that overlies the saline water is about 80 ft thick near the Niagara Escarpment and less than 30 ft thick 8 mi to the south, near the Niagara River.

A natural-gas reservoir in the underlying Clinton Group prevents downward flow of water from the Lockport Group. The gas pressure is 5 to 100 psi greater than the hydrostatic pressure in the horizontal-fracture zones and results in an upward gradient at the base of the Lockport Group. The presence of gas in horizontal-fracture zones in the Gasport Limestone at piezometers 13–17 and 04–20 (fig. 4, p. 12) suggests that high-angle fractures connect the Lockport Group with the gas reservoir in the Clinton Group.

GROUND-WATER FLOW MODEL

Ground-water flow through the aquifer was simulated with a three-dimensional, finite-difference model in which model layers correspond to horizontal-fracture zones, and vertical leakage represents flow through high-angle fractures.

Model Design

The model was constructed with the computer program MODFLOW developed by McDonald and Harbaugh (1988). Because the local variation in transmissivity within a fracture zone was assumed to be small in relation to the model-grid spacing, the fracture network within each horizontal-fracture zone represents a virtually isotropic, homogeneous, porous medium. Although aquifer-test results have shown that local variations in transmissivity within a fracture zone can greatly affect the direction and rate of ground-water flow at a scale of tens to hundreds of feet, the effects of such variations at the 1,000-ft cell size specified in the model are assumed to be negligible.

Model Layers and Grid

The stratigraphic units shown in figure 2 were represented by 10 model layers. Model layers 1, 2, and 3 represent the glacial sediments that overlie the bedrock, the weathered bedrock, and the Salina Shale (which overlies the Lockport Group in the southern part of the modeled area), respectively. The Guelph Formation of the Lockport Group was represented by model layers 4 and 5. The nine regional water-bearing zones within the Lockport Group were represented by five model layers (layers 6–10, fig. 2). These layers correspond to one or more stratigraphic units within the Lockport Group, and the top and bottom of each layer were generally chosen to coincide with a stratigraphic contact. The horizontal-fracture zones generally lie along these contacts, but some fractures are within the units as well. The two massive (unfractured) units in the Lockport Group were represented by decreased vertical conductance between the layers above and below them.

Each of the 10 model layers was divided into a uniformly spaced grid of 1,000 ft, with 71 rows and 69 columns. The model represents an area of 110 mi^2 and contains 3,065 active cells (fig. 4). The grid was oriented N. 50°E. so that the rows and columns were subparallel to the strike of joint sets observed in bedrock outcrops by Gross and Engelder (1991). This alignment allowed for simulation of horizontal anisotropy within horizontal-fracture zones that could be related to channels formed by increased dissolution at their intersections with the high-angle joints. This feature was incorporated in an alternative model, described later.

The weathered bedrock was assumed to be a continuous water-bearing zone that extends throughout the modeled area. The underlying fracture zones rise to the north, where they are truncated by the weathered bedrock (fig. 5). The parts of model layers that correspond to subcrop areas within the weathered bedrock were delineated by projecting the top and bottom of each layer along the regional dip to their points of intersection with the bedrock surface (fig. 6). Parts of the model layers that were projected updip of the bedrock surface or within subcrop areas were assigned zero transmissivity and an extremely high vertical hydraulic conductivity to maintain the hydraulic connection between the weathered bedrock and underlying layers. Model cells in these areas, although active, did not affect the calculation of hydraulic head in the model. Transmissivity values in parts of the model layers that pinch out beneath the weathered bedrock were decreased by a factor (see b'/b

in fig. 6) to account for the decreasing layer thickness in these areas.

Boundary Conditions

The lateral boundaries of the modeled area were chosen to correspond with natural hydrologic boundaries, including the Niagara Escarpment and the Niagara River Gorge. Where no natural hydrologic boundaries were present, no-flow or constant-head boundaries were placed in accordance with potentiometric-surface maps of each model layer. Several manmade structures were also represented as boundaries within the modeled area.

Boundary conditions were specified in model layers 1 and 2 to represent vertical flow between the weathered bedrock and land surface (fig. 6). Constant-head boundaries in model layer 1 represented water levels in the Niagara River and perennial streams. The remainder of model layer 1 was inactive, with no horizontal flow. The area where the river directly overlies the weathered bedrock near Niagara Falls (fig. 3A) was represented by a constant-head boundary in model layer 2. Recharge to the weathered bedrock was specified in the remainder of model layer 2 and was assumed to be inversely proportional to the thickness of the overlying glacial sediments.

Head-dependent boundaries were specified in model layer 2 to represent lateral flow to and from the weathered bedrock along the Niagara Escarpment to north of the modeled area and the Canadian border to the southwest (fig. 7, p. 15). No-flow boundaries were specified along the eastern and southern boundaries to represent streamlines in the weathered bedrock, as depicted in figure 3A. A drain was specified to represent flow to the Niagara River Gorge along the western boundary.

Constant-flow boundaries were specified in the lower model layers (layers 3–10) to represent underflow from upgradient areas south of the modeled area. The flow rates were estimated from (1) the Darcy equation, (2) transmissivity computed from slug tests, and (3) the measured hydraulic gradient. Flow to the Niagara River Gorge was represented by drains as in model layer 2. The other lateral boundaries in the lower model layers and the bottom boundary beneath layer 10 were specified as no-flow. These boundaries represent the approximate location of streamlines along the eastern and western sides of the modeled area and the gas reservoir that restricts vertical flow to or from the bottom of the Lockport Group.

Manmade structures represented in the model include the NYPA hydropower-project facilities (intakes, conduits, forebay canal, and reservoir), industrial wells, and tunnels and airshafts excavated in the bedrock within the city of Niagara Falls (fig. 1). The excavations were represented by drains where they intersected model layers. The transmissivity values used to compute the conductance of the drains were assumed equal to that of the horizontal-fracture zones. Constant-head boundaries were specified at the NYPA reservoir (layer 1) and the forebay canal (layer 10). The extensive drain system surrounding the NYPA conduits was represented by model cells with a transmissivity of 10^6 ft^2/d, estimated from (1) the Darcy equation, (2) the measured flow entering the Falls Street tunnel from the conduit drain, and (3) the measured hydraulic gradient along the conduit drain. Pumpage from industrial wells represented in the model is shown in table 3.

The conductance, C, in model cells representing the head-dependent and drain boundaries was computed from the relation

$$C = \frac{Tw}{l} \qquad (1)$$

where T is cell transmissivity (LT^{-2}),
w is cell width (L), and
l is length of flow path between cell center and the model boundary (L).

The transmissivity of the weathered bedrock was used to compute the conductance of the head-dependent boundaries in model layer 2. An arbitrary transmissivity value of 10^4 ft^2/d was used to compute the conductance of the drain boundary representing the Niagara River Gorge to form an essentially constant-head boundary through which only discharge could occur.

Table 3. Pumpage from industrial wells simulated in the Niagara Falls model

[Well locations shown in fig. 1]

Location	Number	Pumpage (cubic feet per day)
Olin Buffalo Avenue plant	1	130,000
Necco Park landfill	2	2,500
Reichold-Varcum Chemicals	3	1,500
Carborundum Specialty Products	4	670

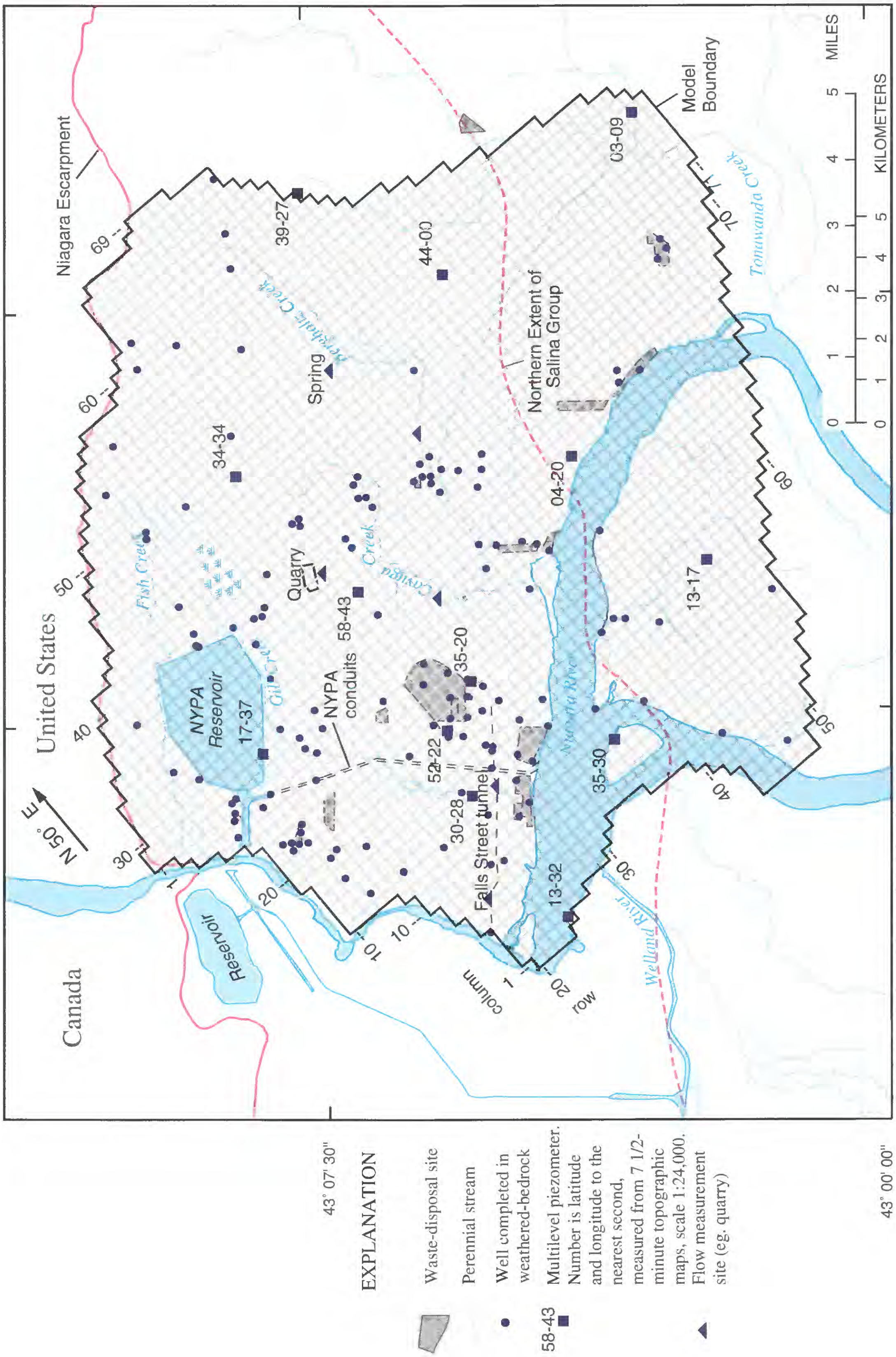

Figure 4. Model grid and locations of wells, multilevel piezometers, and streamflow-measurement sites in the Niagara Falls area.

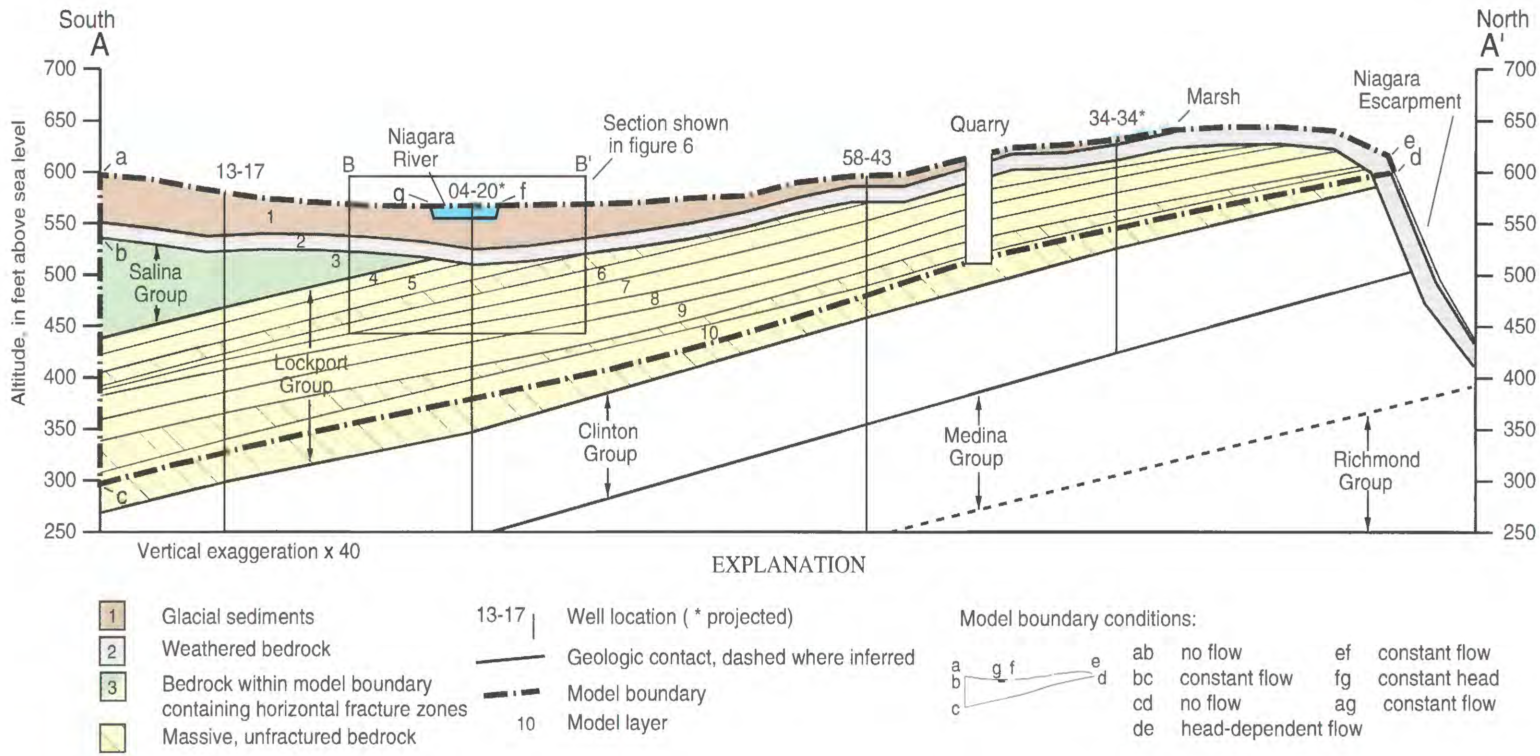

Figure 5. Generalized section A–A′ showing extent of model layers and model boundary conditions. (Location of section is shown in fig. 7, p.15.)

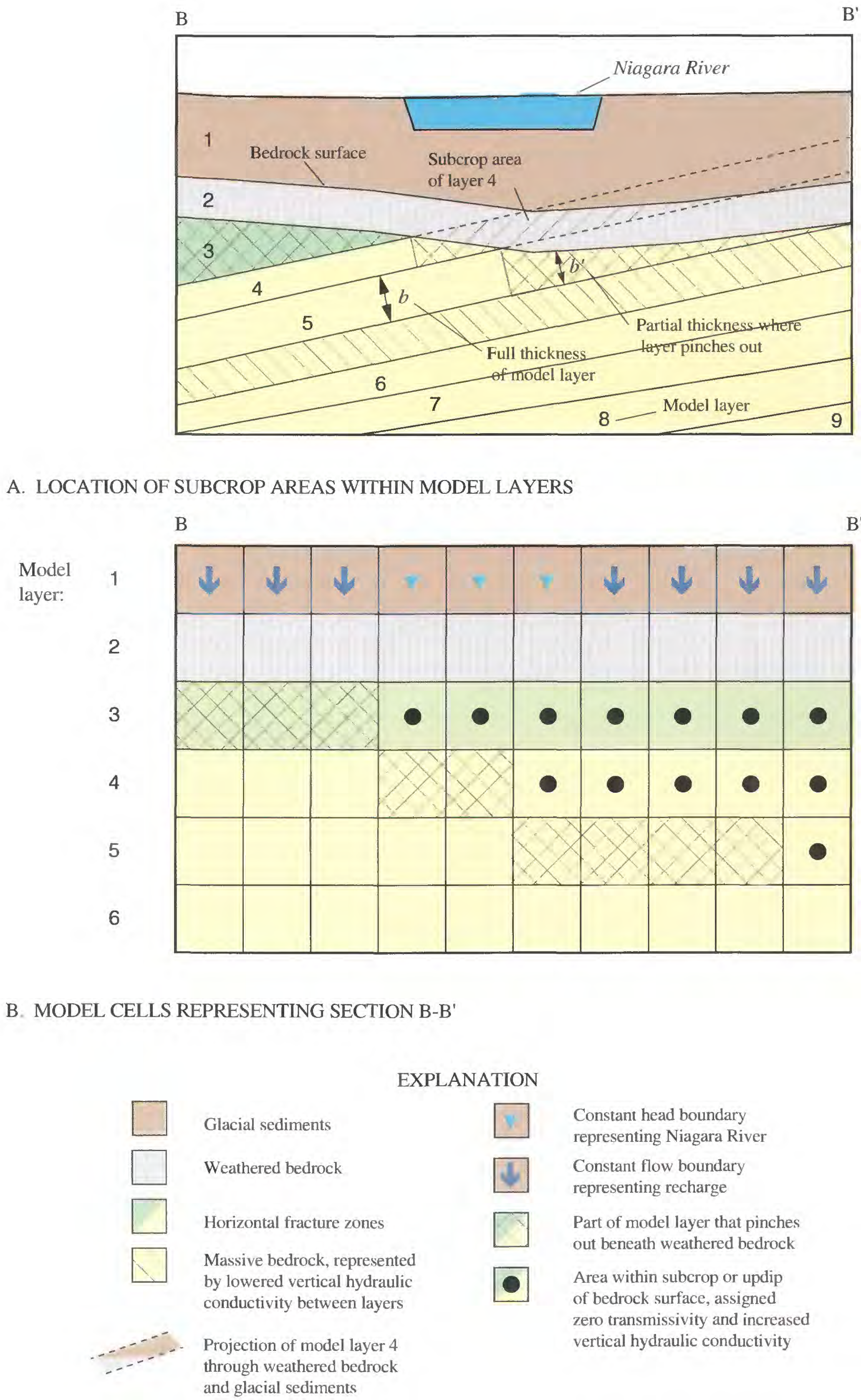

Figure 6. Schematic diagrams of section B–B′ showing: A. Location of subcrop areas within model layers. B. Representation in model.

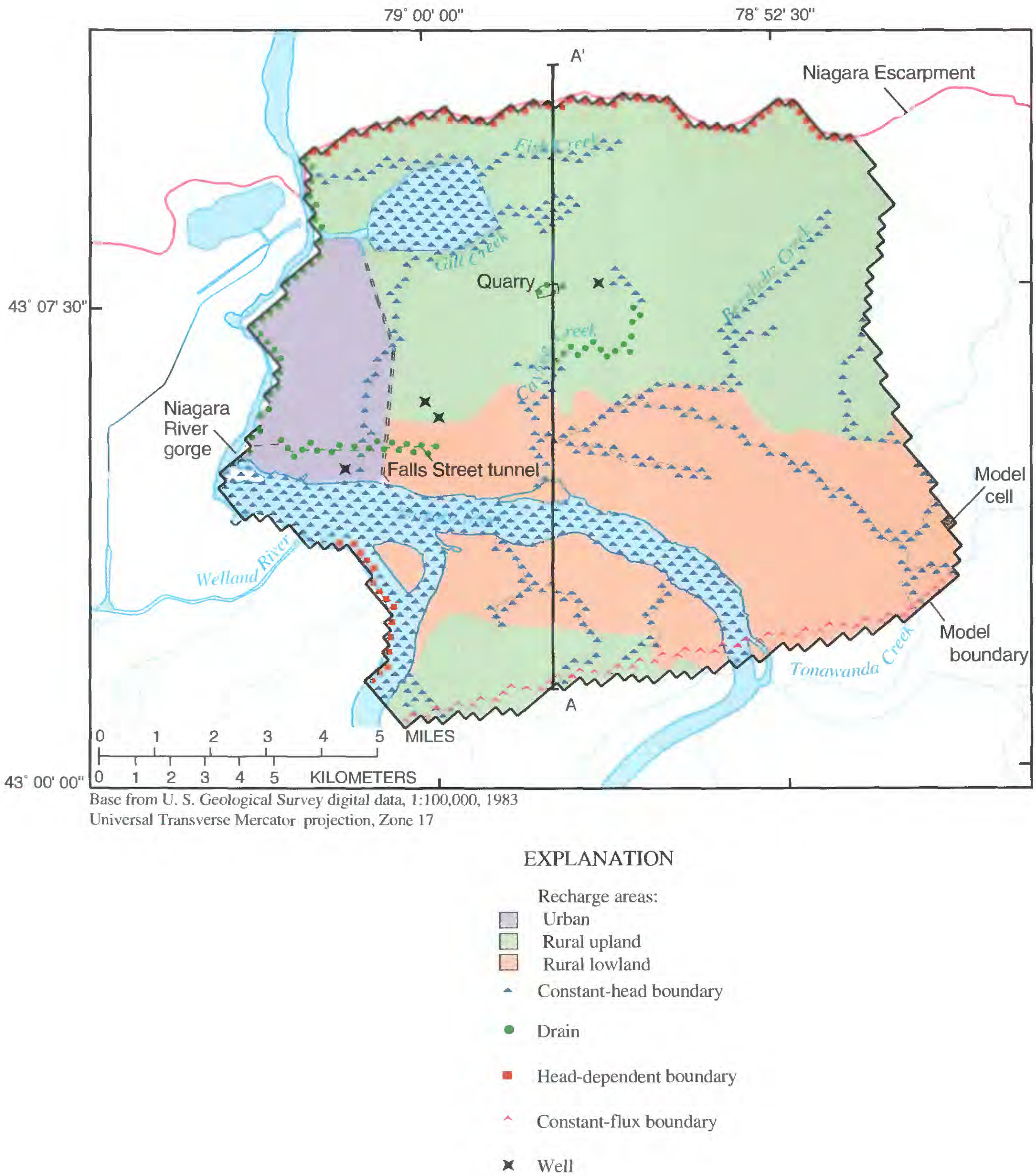

Figure 7. Boundary conditions within the modeled area.

MODEL CALIBRATION

Average steady-state conditions were assumed for the modeled area because hydraulic structures that affect flow have been in place about 30 years, and because well hydrographs show no long-term trends in water levels (Miller and Kappel, 1987). Results of the model simulations were compared with (1) 144 measurements of hydraulic head in weathered-bedrock wells, (2) 64 pressure measurements in the horizontal-fracture zones from 13 multilevel piezometers, (3) low-flow measurements of a spring and two streams, and (4) two discharge measurements along the Falls Street tunnel and one measurement near the Niagara Falls quarry [(fig. 4, and table 7 (p. 22)]. The pressure measurements made in the horizontal-fracture zones were converted to freshwater hydraulic head. The effects of variable density on ground-water flow through the lower part of the Lockport Group were beyond the scope of study and were not included in the model.

Calibration Procedure

Parameter values representing hydraulic properties of the aquifer and model boundary conditions were adjusted during model calibration to produce a model that could approximate the 214 measurements of head and flow. Model parameters were estimated through a nonlinear-regression method developed by Cooley and Naff (1990) and modified for application with MODFLOW by Hill (1992). The method finds parameter values that minimize the sum of squared errors (*SSE*) for a model based on a set of assumptions about the aquifer system, where *SSE* is defined as follows:

$$SSE = \Sigma[w_i^{1/2} e_i]^2, i = 1, n \qquad (2)$$

where e_i is the difference between the observed and calculated values of measurement i,

$w_i^{1/2}$ is the square root of the weight assigned to the error in the observed value of measurement i;

$w_i^{1/2}e_i$ is the weighted residual corresponding to measurement i; and

n is the number of observations.

The resulting parameter values are called the optimal parameter values for the set of assumptions considered.

Improvements in model results were also identified through a comparison of the standard error of estimate (Draper and Smith, 1981, p. 207, herein referred to as standard error, (*SE*) for different models, where *SE* is defined as follows:

$$SE = \left[\frac{SSE}{n-p}\right]^{1/2} \qquad (3)$$

where p is the number of model parameters estimated by the regression.

The nonlinear regression method computes scaled sensitivities that equal

$$\frac{\partial y_i}{\partial b_j} w_i^{1/2} b_j, i = 1, n; j = 1, p \qquad (4)$$

where b_j is one of the model parameters, and

y_i is a measurement of hydraulic head or flow

The scaled sensitivities computed for different model parameters can be compared to determine the relative effect of each parameter in the regression. In general, parameters with scaled sensitivities several orders of magnitude less than other parameters have little effect on simulated results and cannot be estimated by regression.

The weights, w_i, were chosen according to procedures in Hill (1992) to reflect the assumed reliability of the measurements and to account for the different units associated with head measurements (L) and flow measurements (L^3/T^{-1}). The square root of the weight for the 156 head measurements made during 1987–92 by the USGS for this study or by other investigators for site-specific studies was assigned a value of 1.0. The square root of the weight of head measurements in 52 wells obtained from the USGS Ground-Water Site Inventory data base was assigned a smaller value (0.7) to reflect the lower reliability of the data. The flow measurements range from 4,000 to 930,000 ft^3/d, and the error is expected to represent at least 5 percent of the flow. Therefore, errors of 200 to 47,000 ft^3/d are expected, and the weights assigned to the flow measurements (table 7, p. 22) were much smaller than those assigned to the head measurements.

The regression procedure ensures that optimal parameter values are obtained for a given set of assumptions about the aquifer system. The remaining error can be ascribed to the use of incorrect assumptions concerning the model design rather than nonoptimal parameter values. The model can then be changed by, for example, incorporating different boundary conditions, changing the values of nonestimated parameters, or adding parameters in an attempt to reduce *SSE* further and improve model fit. The nonlinear regression also provides estimates of the reliability of estimated values and the correlation between model parameters. This information is used to improve the calibration through (1) identification of parameters to which the model was insensitive, and (2) grouping of correlated parameters.

The number of parameters specified in the model is summarized in table 4. Hydraulic properties of the aquifer system were represented by 27 model parameters, and an additional 6 parameters were specified to represent manmade structures. Initial simulations were conducted to determine the sensitivity of model-computed heads and flows to changes in the parameter values representing aquifer properties. The number of model parameters estimated during calibration was then decreased by assigning fixed values to those parameters to which the *SSE* was insensitive; for example, the transmissivities of model layers 3 to 5 representing the Vernon Shale and the Guelph Dolomite (fig. 2). The number of parameters was decreased further by grouping those that were likely to be affected by the same geologic processes. For example, the transmissivities of model layers 6 through 10, which represent the nine regional horizontal-fracture zones (fig. 2), were replaced by a single parameter representing the transmissivity of a single fracture zone because the range of transmissivity values estimated from hydraulic tests was relatively small. The transmissivity of each layer was then obtained by multiplying this parameter by the number of fracture zones represented by the layer. The calibrated parameter set representing the aquifer system contained 15 values, 7 of which were estimated through calibration. The other parameters representing aquifer properties, and the parameters representing manmade structures, were held constant during the regression.

Estimates of Aquifer Properties

The values of the seven aquifer properties estimated by nonlinear regression (table 4) are listed in table 5. In the regression, transmissivity and vertical hydraulic conductivity were log-transformed to ensure that the estimated values remained positive (Hill, 1992). Transmissivity values were also estimated for model boundaries representing the Niagara Escarpment and the Niagara River Gorge, but optimal values were not obtained because the regression procedure did not converge when these parameters were included in the regression. Apparently, the *SSE* was insensitive to these parameters as long as the values were close to the fixed value specified in the calibrated parameter set.

Transmissivity

The transmissivity of the weathered bedrock was estimated to be 220 ft^2/d—a value less than the median value estimated from hydraulic tests conducted in this study (600 ft^2/d) in which a saturated thickness of 15 ft is assumed, but within the range of reported values for aquifer tests (20 to 3,000 ft^2/d). Transmissivity in reaches along the Niagara riverbed where the bedrock crops out (fig. 3A) was assumed to be 2,000 ft^2/d, in accordance with results of an aquifer test conducted in this area by Legette, Brashears and Graham, Inc. (1979).

The transmissivity of each horizontal-fracture zone within the Lockport Group was estimated to equal 99 ft^2/d, nearly the median value obtained from hydraulic tests (100 ft^2/d). The transmissivity in parts of model layers where the depth below the bedrock surface exceeded 80

Table 4. Parameters representing aquifer properties specified in the Niagara Falls model

[Dash indicates no estimate was made]

Model Parameter	Number in initial set	Number in calibrated set	Number estimated by nonlinear regression
Transmissivity	11	5	2
Vertical hydraulic conductivity	11	4	3
Hydraulic conductivity at boundaries	4	3	-
Recharge	1	3	2
Total	27	15	7

Table 5. Estimates of aquifer properties obtained through nonlinear regression

[ft^2/d = feet squared per day; ft/d = feet per day]

Property	Value
Transmissivity*, ft^2/d:	
weathered bedrock	220
horizontal fracture zones	99
Vertical hydraulic conductivity*, ft/d:	
glacial sediments	6.6×10^{-3}
weathered bedrock	1.3×10^{-2}
unweathered bedrock	1.1×10^{-3}
Average recharge rate, ft/d:	
urban areas	2.5×10^{-3}
rural areas	1.2×10^{-4}

*Log-transformed parameter values.

ft was decreased by a factor of 100 to reflect the finding that fractures are generally closed at these depths, in accordance with results of slug tests conducted in individual fracture zones and discussed earlier. In the bottom model layer, which represented the Gasport Limestone, a depth of 150 ft was used to delineate areas of low transmissivity because open fractures were penetrated at depths below 80 ft in this unit.

The maximum transmissivity of the entire Lockport Group can be obtained as the sum of the transmissivity of the model layers. The model layers represent the weathered bedrock and nine regional fracture zones; therefore, the maximum transmissivity is

$$220 + (9 \times 99) = 1{,}100 \text{ ft}^2/\text{d}.$$

The transmissivity is less than this value in many parts of the modeled area that contain fewer than nine regional fracture zones. In the northern part of the area near the Niagara Escarpment, for example, the Lockport Group is thinner and the stratigraphic contacts fewer than in the southern part, where the depth to several of the stratigraphic contacts exceeds 80 ft, and the transmissivity of individual fracture zones is less than 1 ft^2/d. The maximum transmissivity of the Lockport Group, excluding the weathered bedrock, is 890 ft^2/d, greater than the median value of 700 ft^2/d computed from slug and constant-head injection tests conducted in 27 boreholes within the modeled area. (Values ranged from 1 to 1,800 ft^2/d.)

Vertical Hydraulic Conductivity

The vertical hydraulic conductivity of the glacial sediments in the modeled area was estimated to be 6.6 x 10^{-3} ft/d, except beneath the NYPA reservoir in Niagara Falls, where it is assumed to be lower by a factor of 10 as a result of consolidation of the sediments during construction of the reservoir. The unconsolidated sediments beneath the Niagara River have the same origin as the glacial sediments and were therefore assigned the same value of vertical hydraulic conductivity. This value is somewhat greater than the median hydraulic conductivity value (2.0 x 10^{-3} ft/d) mentioned earlier but is within the range of reported values (2 x 10^{-5} to 9 x 10^{-1} ft/d).

The vertical hydraulic conductivities of the weathered bedrock and of the unweathered bedrock that separates the horizontal-fracture zones in the Lockport Group were estimated to be 1.3 x 10^{-2} ft/d and 1.1 x 10^{-3} ft/d, respectively. These values represent the effective vertical hydraulic conductivity of a network of high-angle fractures between (1) the weathered bedrock and underlying horizontal-fracture zones, and (2) between adjacent fracture zones, respectively. The vertical hydraulic conductivity along bedrock outcrops, where the density of joints is assumed to have increased through stress-release fracturing, was specified to be 10 times higher. To determine the effective horizontal-to-vertical anisotropy of the unweathered bedrock in model layers 6 through 10, each layer was considered to be about 15 ft thick and to contain two fracture zones, on average. The transmissivity of two fracture zones equals 198 ft^2/d; dividing this by 15 ft yields an effective horizontal conductivity of 13 ft/d and an effective anisotropy of 12,000:1. This ratio is much higher than the 70:1 ratio estimated from results of cross-hole tests, but the cross-hole tests were conducted within an area assumed to contain a greater density of high-angle fractures than other areas. No other estimates from field tests are available for comparison.

Recharge

The modeled area was divided into two zones—an urban zone and a rural zone consisting of an upland and a lowland zone (fig. 7)—and the rate of recharge to the weathered bedrock in each was estimated. The zones were delineated according to surface-drainage characteristics that could affect the rate of recharge. The urban zone was within the city of Niagara Falls west of the NYPA conduits, where the percentage of impervious surfaces is greater than in other areas and produces a greater volume of surface runoff. The surface runoff flows through storm sewers, which are brick-lined tunnels that intersect the bedrock near topographic highs; therefore storm runoff could enter the weathered bedrock directly in these areas. Another source of recharge could be conveyance loss from the municipal water supply; this is estimated to total 13.6 Mgal/d or an average of 28 in/yr over the urban area (G.H. Grose, City of Niagara Falls, oral commun., 1992).

The rate of recharge to the weathered bedrock in each model cell was computed by dividing the maximum recharge rate estimated through regression by the thickness of the overlying glacial sediments in each cell. Thus, the actual recharge rate in each model cell was inversely related to sediment thickness. This is consistent with Darcy's law:

$$q = k_v i \qquad (5)$$

unit area (L/T $^{-1}$),

k_v is vertical hydraulic conductivity (L/T $^{-1}$), and

i is the hydraulic gradient, $\Delta h/\Delta l$ (dimensionless).

When recharge to the weathered bedrock is computed through equation 5, Δl equals the vertical difference between the water table and the bottom of glacial sediments, and Δh equals the difference in hydraulic head between the weathered bedrock and the water table in the glacial sediments. If the weathered bedrock is a confined aquifer and the glacial sediments are saturated, then the maximum possible difference in hydraulic head (Δh) equals Δl, and the vertical hydraulic gradient is equal to 1. In this situation, the maximum possible recharge equals the vertical hydraulic conductivity of the glacial sediments. The maximum recharge rate calculated from the median value of reported vertical hydraulic conductivity mentioned earlier (2×10^{-3} ft/d), is about 9 in/yr, and the maximum rate calculated from the calibrated value (6.6×10^{-3} ft/d) is 29 in/yr.

The mean recharge rate in each area (reported in table 5) was obtained as the sum of the recharge to each model cell, divided by the number of cells. The mean recharge rate in the urban and rural areas were estimated by regression to be 2.5×10^{-3} ft/d (11 in/yr) and 1.2×10^{-4} ft/d (0.5 in/yr), respectively. The largest recharge rate in the urban area was 5.3×10^{-3} (23 in/yr), more than twice the maximum rate of 2.1×10^{-3} ft/d (9 in/yr) calculated from the median hydraulic conductivity, but less than the maximum rate of 6.6×10^{-3} ft/d (29 in/yr) calculated from the calibrated value. The lower recharge rate yielded hydraulic-head values 40 ft less than those observed in the urban area, which indicates an additional source of recharge in this zone. The possible sources are conveyance losses from the municipal water supply and surface runoff from storm sewers.

Hydraulic-Head Distribution

The hydraulic-head distribution in the weathered bedrock computed by the calibrated model is similar to that contoured from the observed data (fig. 3A) and indicates that ground water flows from topographic highs near the escarpment toward the Niagara River and its tributaries and toward the NYPA conduits (fig. 8A). Within the city of Niagara Falls, ground water flows from topographic highs near the center of the urban area toward discharge boundaries that surround the city—the Niagara River Gorge, forebay canal, NYPA conduits, and Falls Street tunnel. The relatively small standard error of 8.9 ft (eq. 3) between hydraulic heads computed for the weathered bedrock and those observed in wells, and the error of less than 10 ft at most wells (fig. 9A), indicates that the model simulates the head distribution reasonably well on a regional scale. The highest observed values of hydraulic head were underestimated by as much as 30 ft in recharge areas near the Niagara Escarpment and in the city of Niagara Falls near the forebay canal (fig. 8A), but in other areas, the model-generated heads were similar to the observed values.

The distribution of computed hydraulic heads in deep model layers parallel those in the overlying weathered bedrock (fig. 8B). The standard error between hydraulic heads computed by the model and those observed in piezometers is also about 10 ft, and the histogram of model error (fig. 9B) indicates a slight bias toward overprediction in the underlying fracture zones. The maximum error is in the bottom model layer, which represents the Gasport Limestone, primarily in recharge areas near the Niagara Escarpment and in discharge areas near Niagara Falls and the NYPA reservoir. The overall predicted distribution of hydraulic head matches the observed distribution reasonably well, however, except for a large concavity on the potentiometric surface contoured from observed data southwest of the Niagara Falls quarry (fig. 3B). The deviation in the observed surface from the smooth hydraulic gradient predicted by the model indicates that this fracture zone contains local variations in transmissivity that are not represented in the model.

Rate of Ground-Water Flow

Rates of flow to and from the modeled area were obtained as the sum of the contributions from each model cell within recharge areas and along discharge boundaries. Recharge accounts for more than 60 percent of the ground water entering the modeled area; infiltration from the Niagara River and the NYPA reservoir accounts for most of the remainder (table 6). About 70 percent of all recharge enters in the city of Niagara Falls, and the rest enters mainly in upland areas. About 25 percent of the water exiting the modeled area discharges to the Falls Street tunnel; the other principal discharge areas are the Niagara River, its tributaries, and the industrial wells.

Computed discharges were compared with six observed discharges, as discussed in the model-calibration section. The computed discharges were within 60 percent of the observed discharges except at the intersection of the Falls Street tunnel with the NYPA conduits (table 7); the computed discharges were less than observed discharges in four areas and exceeded them at two—Bergholtz Creek and the Falls Street tunnel downstream of the NYPA conduits (fig. 4). The discrepancy between the computed and observed values is probably due to local variation in transmissivity within the bedrock that is not represented by the model. For example, the measured base flow per unit area in the Bergholtz Creek watershed is equivalent to about 0.03 $(ft^3/s)/mi^2$ or one-quarter that of the Cayuga Creek watershed (0.12 $(ft^3/s)/mi^2$). The regression attempted to match both of these measured flows and, as a result, overpredicted flow to Bergholtz Creek and underpredicted flow to Cayuga Creek.

The largest discrepancy in volume of flow was at the intersection of the Falls Street tunnel with the NYPA conduits, where predicted discharge was less

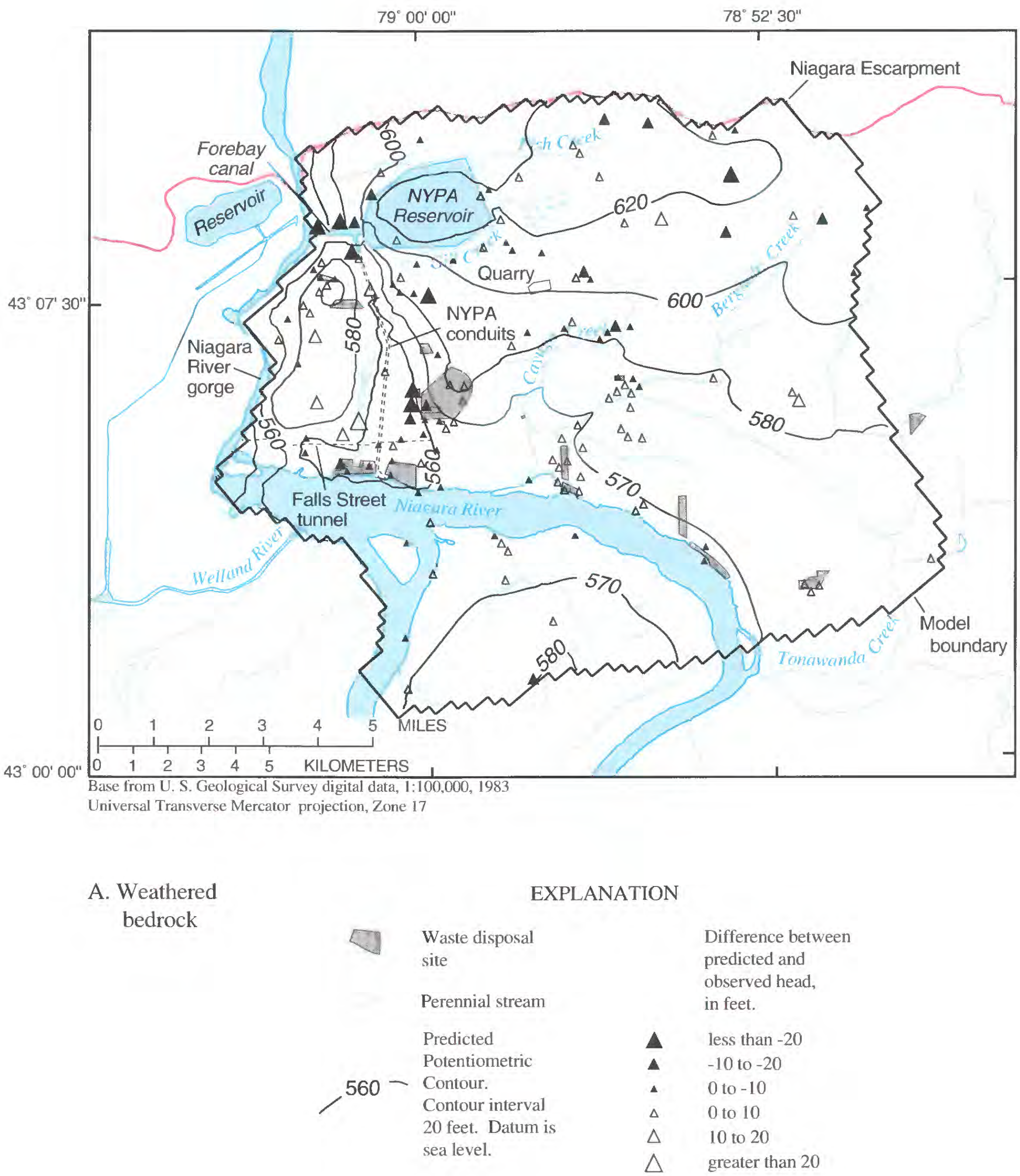

Figure 8A. Hydraulic-head distribution in the weathered bedrock, as computed with the calibrated model.

than half the observed flow of 930,000 ft^3/d (7.0 Mgal/d), even though about one quarter of the ground-water flow from the entire modeled area was draining to the tunnel. This result suggests that an additional source of water not represented in the model is contributing much of the flow. The Niagara River could provide enough water to match the observed flow if a path of high transmissivity were present between the river and the tunnel or the NYPA conduit drain. Possible paths include the coarse backfill materials (shot rock) surrounding the conduit intakes and(or) leaks in the grout curtain surrounding the intakes; alternatively, a

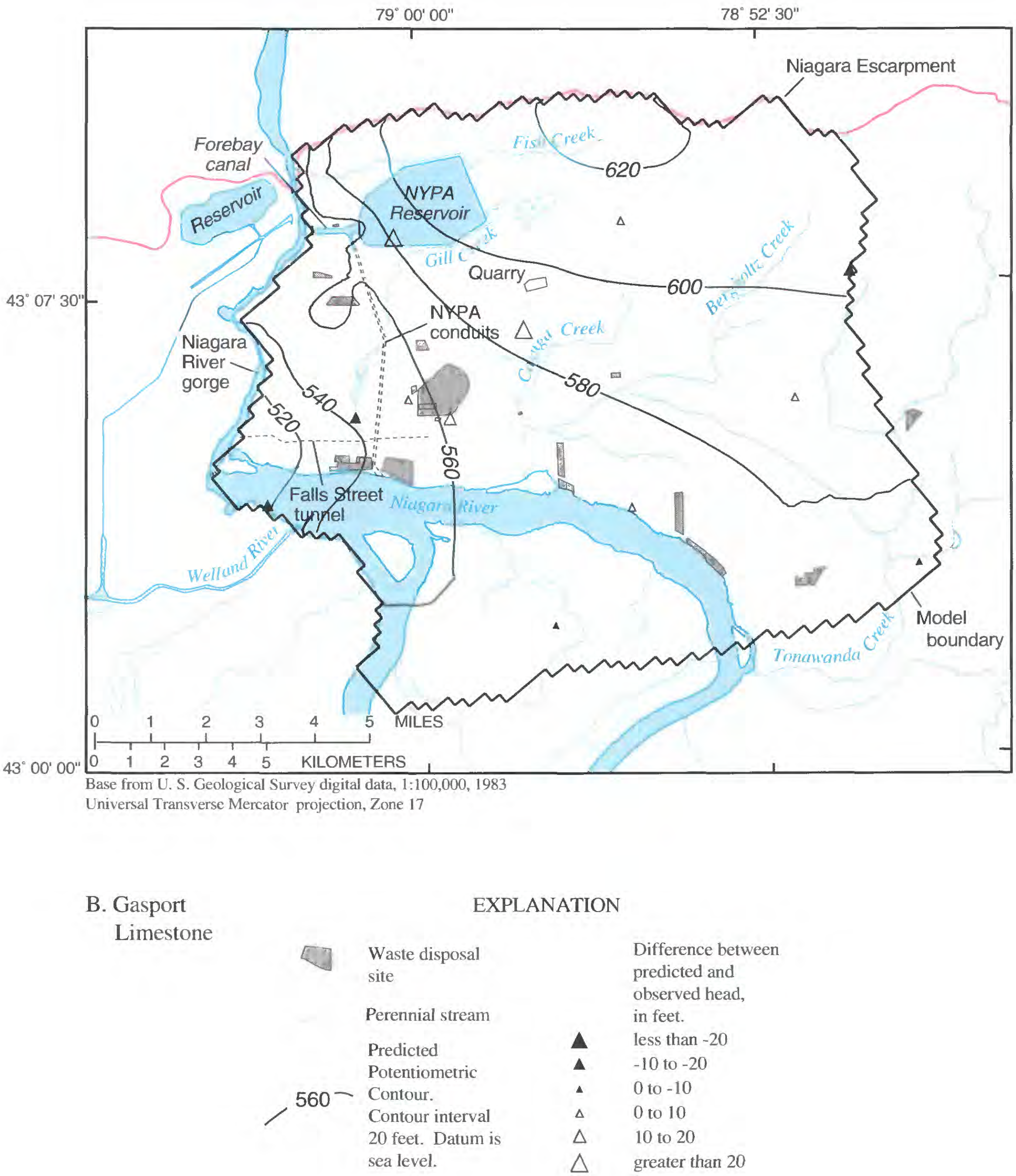

Figure 8B. Hydraulic-head distribution in the Gasport Limestone, as computed with the calibrated model.

highly fractured zone might intersect the tunnel or conduit drains. A narrow band of high-yielding wells extending from the river to the tunnel/conduit intersection identified by Johnston (1964) supports this latter hypothesis (Yager and Kappel, 1987).

Discharges of ground water to the Falls Street tunnel at an airshaft near 18th Street and to Cayuga Creek at a sewer lift-station near Lockport Road were not included as observed values in computations of the sum-of-squared errors of the nonlinear regression because these large flows probably emanate from highly fractured karst features that have developed in the Lockport Group near manmade structures and therefore are not representative of average discharges from the bedrock. Actual ground-water discharges from the modeled area are 5.5 Mgal/d larger than those computed from the model results, including contributions from these two flows and the underestimated flow to the Falls Street tunnel at the NYPA conduits (3.5 Mgal/d); this indicates that inflows to the bedrock are also larger than those estimated by the model. Most of this inflow is probably derived from the Niagara River near the city of Niagara Falls, and the remainder is probably recharge through the glacial sediments.

Table 6. Simulated water budget for the Lockport Group under average steady-state conditions
[Flow rates are in thousands of cubic feet per day]

Inflow	Rate	Percentage of total	Discharge	Rate	Percentage of total
Recharge	1,100	61	NATURAL AREAS:		
NYPA reservoir	280	16	Niagara River Gorge	530	30
Niagara River	270	15	Tributaries	330	19
Tributaries	130	7	Niagara River	94	5
Underflow	13	1	Niagara Escarpment	40	2
			MANMADE STRUCTURES:		
			Falls Street tunnel at NYPA conduits	450	25
			Industrial wells	130	7
			Tunnels	150	8
			Excavations	67	4
TOTAL	1,800	100		1,800	100

Table 7. Ground-water flow rates measured in selected discharge areas and computed with the calibrated model
[Flow rates are in cubic feet per day (ft^3/d). Locations are shown in fig. 4]

Discharge area	Observed flow	Calibrated model flow	Weight ($w^{1/2}$) assigned to observed flow in regression
Intersection of Falls Street tunnel with NYPA conduits	930,000	380,000	5.4×10^{-5}
Remainder of Falls Street tunnel[1]	70,000	73,000	7.1×10^{-4}
Cayuga Creek[2]	40,000	24,000	1.3×10^{-3}
Bergholtz Creek	32,000	49,000	1.6×10^{-3}
Niagara Falls quarry	13,000	8,000	3.9×10^{-3}
Perennial spring	4,000	2,400	1.3×10^{-2}

[1] Does not include 200,000 ft^3/d entering airshaft near 18th Street.

[2] Does not include 70,000 ft^3/d entering creek from sewer lift-station near Lockport Road.

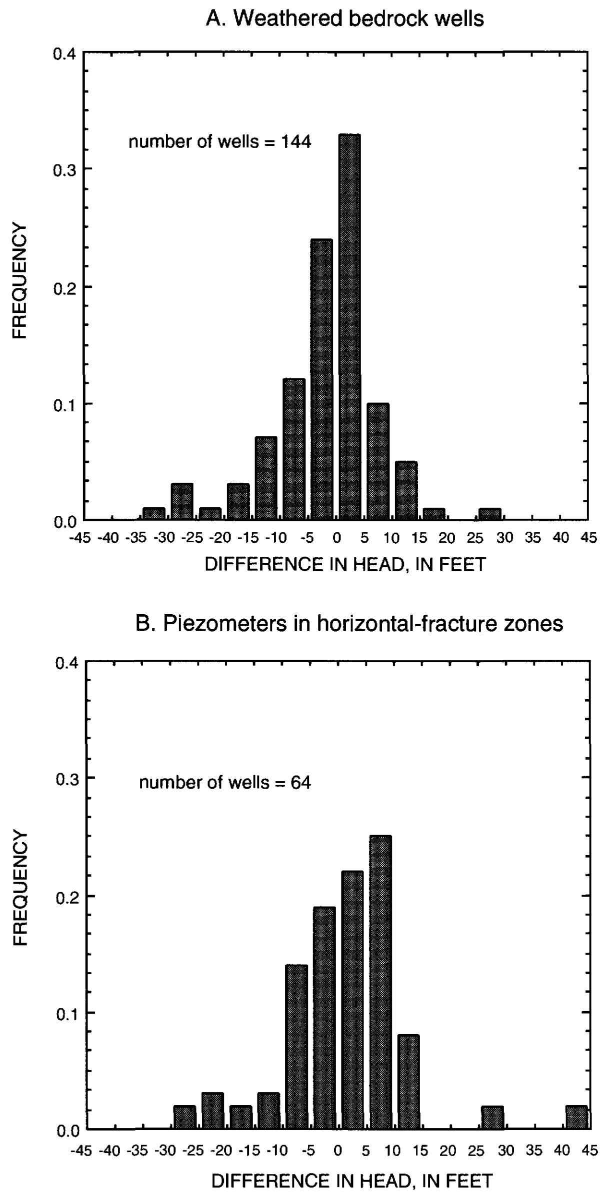

Figure 9. Differences between predicted and observed heads in (A) weathered bedrock wells, and (B) piezometers in underlying fracture zones.

Alternative Models

The nonlinear-regression procedure was used to estimate optimal parameter values for the model. Modifying the values increases the model error (as measured by *SSE* and *SE*). For example, when the transmissivity of the weathered bedrock and of the horizontal-fracture zones was decreased by one-half, the *SSE* increased by 20 percent, and when the recharge rate in the city of Niagara Falls was decreased by one-half, the *SSE* increased by 32 percent. Apparently, to change the value of parameters without significantly increasing the *SSE* would require a different model design with different boundary conditions or distribution of parameter values. To determine whether the aquifer system could be represented by other equally plausible model designs, three alternative models with different boundary conditions or parameter distributions from those of the calibrated model were developed, and optimum parameter values were obtained through nonlinear regression for each model. The optimum parameter values for each model are listed in table 8 with the sum of squared errors in heads and flows. Flow rates beneath selected waste-disposal sites in the modeled area were then computed with the calibrated model and the two most plausible alternative models.

The first model included additional zones of recharge (model A), the second included different boundary conditions (model B), and the third included horizontal anisotropy within model layers (model C). In model A, recharge in the rural zone was divided into upland areas characterized by sloping terrain and lowland areas with relatively flat slopes (fig. 7). This caused little change in the *SSE* or the optimal parameter values, except that the mean recharge rate of the lowland area was estimated to be negative, indicating that ground water discharges upward from the weathered bedrock toward land surface in this area. This result is consistent with that of another simulation in which a constant-head boundary was specified in model layer 1 to represent the water table in the glacial sediments. In this simulation, the lowland area was also a zone of ground-water discharge. Data are insufficient to indicate whether ground-water discharge actually occurs in these areas, however.

In model B, the drain conductance along the western boundary representing the Niagara River Gorge was decreased by a factor of 1,000 to determine whether restricting flow to this boundary would alter the parameter values; this decrease in conductance decreased estimated recharge in the urban zone by 40 percent (table 8). The standard error decreased only slightly, but the predicted direction of ground-water flow in the weathered bedrock in the city of Niagara Falls was not westward to the Niagara River Gorge, as would be indicated by the observed hydraulic gradient (fig. 3A).

In model C, horizontal anisotropy of the weathered bedrock was included in the parameter set to represent the possible preferential dissolution of fractures aligned with the prominent joint sets that are subparallel to the model grid. Some of the resulting parameter values differed significantly from those obtained in the other models, and the standard error decreased by 7 percent relative to the calibrated model. The horizontal anisotropy was estimated to be about 20:1 and resulted in a northeast-southwest transmissivity (along model rows) of 1,500 ft^2/d and a northwest-southeast transmissivity (along model columns) of 70 ft^2/d. The estimated vertical hydraulic conductivities of the weathered bedrock and the unweathered bedrock were decreased and increased by a factor of 2, respectively, so that the two values were nearly equal, unlike the values in the other models. The estimated recharge rates in urban and rural areas both increased by about 45 percent relative to those of the calibrated model.

Results of model C suggest that horizontal anisotropy of the weathered bedrock could be significant, but its degree might not be accurately estimated because the correlation between the transmissivity of the weathered bedrock and the recharge rate in the urban area in model C, calculated from their covariance, is 0.89, a strong positive correlation. Also, the scaled sensitivities associated with each parameter have opposite signs; thus, changing the values of the parameters simultaneously does not significantly change the predicted heads. For example, decreasing both the transmissivity of the weathered bedrock and the urban recharge rate in the same simulation would have little effect on model error. In a separate regression, decreasing the maximum transmissivity of the weathered bedrock to the median value (600 ft^2/d) estimated from hydraulic tests conducted in this study resulted in a 40-percent decrease in estimated urban recharge rate and, as expected, little increase in model error. The horizontal anisotropy estimated in this regression was 10:1, much less than the value of 20:1 estimated in model C. This result suggests that additional information on the transmissivity of the weathered bedrock or the urban recharge rate would be required for estimation of horizontal anisotropy with model C.

Table 8. Optimum parameter values obtained through nonlinear regression for alternative model designs and their confidence intervals at 95-percent level for the calibrated model

[ft^2/d = feet squared per day; ft^2 = feet squared; dashes indicate not estimated]

	Calibrated model	Individual confidence interval	Alternative model designs		
			Model A	Model B	Model C
Hydraulic property:					
Transmissivity, ft^2/d					
weathered bedrock	220	120 - 420	150	240	1,500/70*
horizontal-fracture zones	99	59 - 170	130	150	90
Vertical hydraulic conductivity, ft/d					
glacial sediments	$6.6x10^{-3}$	$4.1x10^{-3}$ - $1.1x10^{-2}$	$6.0x10^{-3}$	$5.8x10^{-3}$	$5.9x10^{-3}$
weathered bedrock	$1.3x10^{-2}$	$5.0x10^{-3}$ - $3.3x10^{-2}$	$1.4x10^{-2}$	$1.2x10^{-2}$	$5.0x10^{-3}$
rock matrix	$1.1x10^{-3}$	$4.1x10^{-4}$ - $2.7x10^{-3}$	$9.4x10^{-4}$	$3.9x10^{-4}$	$2.5x10^{-3}$
Average recharge rate, ft/d					
urban areas	$2.5x10^{-3}$	$1.8x10^{-3}$ - $3.2x10^{-3}$	$2.9x10^{-3}$	$1.5x10^{-3}$	$3.7x10^{-3}$
rural areas	$1.2x10^{-4}$	$9.4x10^{-5}$ - $5.7x10^{-3}$	--	$1.3x10^{-4}$	$1.7x10^{-4}$
uplands	--	--	$1.9x10^{-4}$	--	--
lowlands	--	--	$-4.1x10^{-5}$	--	--
Sum of squared errors, ft^2:					
heads	16,600		15,900	15,500	15,000
flows	2,800		2,900	2,600	1,600
Standard error in heads and flows, ft	9.68		9.55	9.35	8.98

* Maximum transmissivity/minimum transmissivity.

Reliability of Estimates

The reliability of parameter values obtained through nonlinear regression can be estimated statistically by computing confidence intervals through methods described by Cooley and Naff (1990) and Hill (1992). These methods require that the model be linear in the vicinity of the optimum set of parameter values and that the parameters be normally distributed. The method also assumes that the model is correct and accurately represents the physical system. Although a model can be shown to be incorrect, to prove that it is correct is generally impossible.

An alternative to the statistical approach for determining which model best represents the flow system is to consider hydrologic information not included in the model, such as whether the predicted flow directions match those interpreted from the potentiometric surfaces shown in figure 3. On this basis, model B can be disregarded because the flow directions in the weathered bedrock in the city of Niagara Falls are not westward to the Niagara River Gorge. The reliability of model A could be tested through comparison of the predicted upward flow in lowland areas with the vertical hydraulic gradients measured between piezometers in the glacial sediments and weathered bedrock, if such data were available. Similarly, the validity of model C could be tested through comparison of the predicted orientation and magnitude of horizontal anisotropy with values obtained from the analysis of several aquifer tests of the weathered bedrock by the method of Papadopulos (1965), as illustrated in Yager and Kappel (1987).

The validity of models A and C cannot be judged from present information; thus, they are as plausible as the calibrated model, although the estimate of horizontal anisotropy obtained with model C is uncertain because of parameter correlation. The errors in predicted heads and flows in these models are slightly less than in the calibrated model because they contain additional parameters. All three models were used to estimate flow rates within the modeled area, including areas beneath the selected waste-disposal sites.

Statistical Analyses

The individual confidence intervals given in table 8 indicate the reliability of the optimal parameter values obtained with the calibrated model. The confidence intervals were computed by the method described in Hill (1992, p. 58) under the assumption that the model is correct and linear in the vicinity of the optimum set of values, and that the parameters are normally distributed. To test model linearity, Beale's measure and its critical values were computed by the methods of Cooley and Naff (1992, p. 187). Beale's measure for the calibrated model was 0.14—below the upper criteria of 0.5 and above the lower criteria of 0.045. This suggests that some degree of nonlinearity is present in the model so that confidence levels for the estimated values computed with standard statistical techniques will be aproximate.

The parameters tend to be normally distributed if the weighted residuals ($w_i^{1/2}e_i$ from eq. 2) are normally distributed and independent, or display a correlation that is expected from the nonlinear regression (Helsel and Hirsch, 1992, p. 225 and 240). The weighted residuals computed with the calibrated model were compared with a normal, independent distribution through two test statistics. The R_N^2 statistic (Hill, 1992, p. 64) for the calibrated model was 0.946, which is less than 0.987, the critical value at the 95-percent confidence level, indicating that the weighted residuals might not be normally distributed. This test is quite restrictive, however; the less powerful Kolmogorov test yielded a D statistic of 0.103, indicating that the weighted residuals are independent and normally distributed at the 99-percent confidence level (Stephens, 1974). Thus, the weighted residuals were judged to be sufficiently close to a normal, independent distribution to suggest that the method of Hill (1992) could be used to estimate confidence intervals for the parameters.

The results of the statistical analyses indicate that the residuals are independent and normally distributed, but some degree of nonlinearity is present in the calibrated model. The apparent bias in the distribution of residuals corresponding to observations in the fracture zones (figs. 8B, 9B) also indicates that the model might be incorrect. For these reasons, the linear confidence intervals presented in table 8 are considered approximate.

Aquifer Properties

The optimal values of most of the parameters in models A and C are within the 95-percent confidence intervals of values estimated with the calibrated model and do not differ by more than 50 percent from the calibrated values (fig. 10). Results of model C suggest, however, that if horizontal anisotropy is significant, the maximum transmissivity of the weathered bedrock is considerably greater than indicated by the calibrated model. Additional estimates of transmissivity could be obtained from aquifer tests in which drawdowns induced

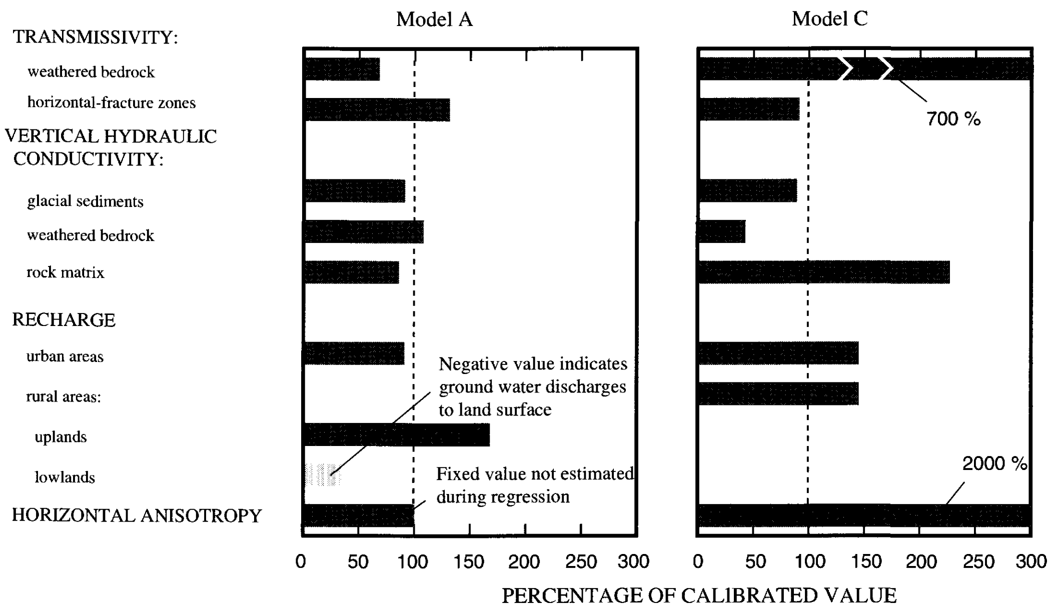

Figure 10. Differences between parameter values obtained by calibrated model and those obtained by alternative models.

by pumping are measured in multiple observation wells, and comparison of the results from several tests in different parts of the study area might indicate whether the weathered bedrock can be treated as an anisotropic porous medium with a consistent direction of maximum transmissivity.

Predicted Heads and Flows

The distribution of hydraulic head and flow rates computed with the model depict average, steady-state conditions in the Lockport Group that might not match the heads and flows at specific points within the modeled area. Differences between predicted and actual conditions are due to the averaging of hydraulic properties over the 1,000-ft grid cells in the model and the treatment of the fracture zones in the Lockport Group as porous media with uniform properties. Another model could be developed with smaller grid cells to more accurately represent the location of streams and manmade structures and provide more detail in the predicted distribution of heads and flows. Despite the small grid spacing, however, the applicability of model predictions at a local scale would still be limited by the assumption of homogeneous, porous media. To accurately predict heads and flows at particular sites, areas of heterogeneity within the fracture zones need to be delineated and estimates of their hydraulic properties obtained.

SIMULATED GROUND-WATER FLOW

Hydraulic heads and flow rates computed by the model were used with a particle-tracking routine developed by Pollock (1989) to generate ground-water flow paths through the modeled area. The tracking technique delineates source areas for discharge boundaries represented in the model by tracing particles from each model cell to a discharge boundary. Horizontal and vertical flow rates within the modeled area were expressed as Darcy velocities (also termed specific discharge) to allow calculation of flow rates through areas that differ in size from the 1,000-ft model cells. The calibrated model and alternative models A and C discussed previously were used to estimate Darcy velocities beneath waste-disposal sites selected by USEPA.

Contributing Areas of Discharge Boundaries

Ground water in rural areas within most of the modeled weathered bedrock discharges to the Niagara River and its tributaries and to the Niagara Escarpment (fig. 11A). Ground water in urban areas discharges to the Niagara River Gorge and manmade structures, including the Falls Street tunnel, a production well at a Buffalo Avenue industrial plant, and the forebay canal. Many waste-disposal sites are within the 10-mi^2

contributing area that drains to the Falls Street tunnel (most of the area discharges to the tunnel at its intersection with the NYPA conduits). About half of the bottom model layer discharges to the Niagara River and its tributaries and the Niagara River Gorge (fig. 11B); the remainder of the bottom layer discharges to the Falls Street tunnel, the industrial production well, and the forebay canal. Most of the contributing area to the Falls Street tunnel enters at its intersection with the NYPA conduits.

Calculation of Darcy Velocity

Horizontal flows within a model layer were computed as the sum of the inflow into each cell through row and column boundaries. The distribution of vertical flow within a layer was taken as the flow through the bottom-cell boundaries. The horizontal and vertical flow rates were converted to Darcy velocities (flow rate per unit area) by dividing them by the cross-sectional flow area of the cell face or by the area of the cell, respectively (fig. 12A). Ground-water flow rates can be computed for areas that differ in size from the 1,000-ft model cells by multiplying the Darcy velocity of the model cell corresponding to the area of interest by the estimated cross-sectional flow area.

Ground-water flow rates beneath 21 waste-disposal sites selected by the USEPA were estimated with the calibrated model and models A and C. The flow rates were estimated with a routine developed by Scott (1990) to compute mean velocity vectors within model cells. The flow rate beneath the waste-disposal sites are also expressed as Darcy velocities (flow rate per unit area) in both the horizontal and vertical directions. The method used to compute the horizontal Darcy velocity differs from that described above to estimate flow rates within model layers, however, in that it also yields the direction of the velocity vector.

A column of model cells extending from the weathered bedrock (layer 2) to the Gasport Limestone (layer 10) was used to estimate the horizontal and vertical Darcy velocities beneath each waste-disposal site (fig. 12B). The horizontal Darcy velocity was computed for the weathered bedrock and the underlying fracture zones, and the vertical Darcy velocity was computed for flow between the weathered bedrock and the underlying fracture zones.

The vertical Darcy velocity through the weathered bedrock was computed as the flow rate through the lower face divided by the area of the cell. Horizontal components of flow along rows and columns of the grid were computed as the average of flows through the front and back faces and the right and left faces of a model cell (fig. 12A). The Darcy velocity along rows and columns was then calculated as the flow components divided by the cross-sectional flow area of the cell face. The two orthogonal flow components were then added to obtain a horizontal vector indicating the direction and magnitude of flow through each cell (fig. 12C). A composite horizontal Darcy velocity through the underlying fracture zones was estimated by averaging the horizontal velocity components of Darcy velocity along rows and columns for all model layers representing the fracture zones. These mean velocity components were then added to obtain a horizontal vector.

Darcy Velocity Within the Lockport Group

Horizontal Darcy velocities through the weathered bedrock range from 10^{-4} to more than 1 ft/d (fig. 13A). Flow rates are higher in urban areas than in rural areas and are highest along the NYPA conduits and near the industrial production well. The smallest horizontal flow rates are near discharge areas in the rural lowlands. Horizontal Darcy velocities through the underlying model layers (fig. 13B) are generally slower than the flow through the weathered bedrock, although rates also range from less than 10^{-4}ft/d to more than 1 ft/d. Again, flow rates are highest in discharge areas along the NYPA conduits and near the Niagara River Gorge. The areas in which flow rates are less than 10^{-3} ft/d generally correspond to areas within the underlying fracture zones that contain saline water. Actual flow rates through these areas are probably less than those predicted by the model because saline water and gas pockets, which are in the underlying fracture zones but not represented in the model, would restrict the flow of freshwater.

Vertical flow within most of the modeled weathered bedrock is downward toward underlying model layers, except in areas adjacent to the Niagara River and its tributaries and the Niagara Escarpment (fig. 14A). Vertical Darcy velocities are smaller than horizontal Darcy velocities and range from less than 10^{-5} to 10^{-2} ft/d. Flow rates are highest in areas of downward flow along the NYPA conduits and beneath the city of Niagara Falls, and in areas of upward flow beneath Cayuga and Bergholtz Creeks, the principal tributaries to the Niagara River within the modeled area. Vertical flow is primarily downward, toward the bottom model layer, in urban areas and the rural uplands (fig. 14B) and is upward

A. Weathered bedrock

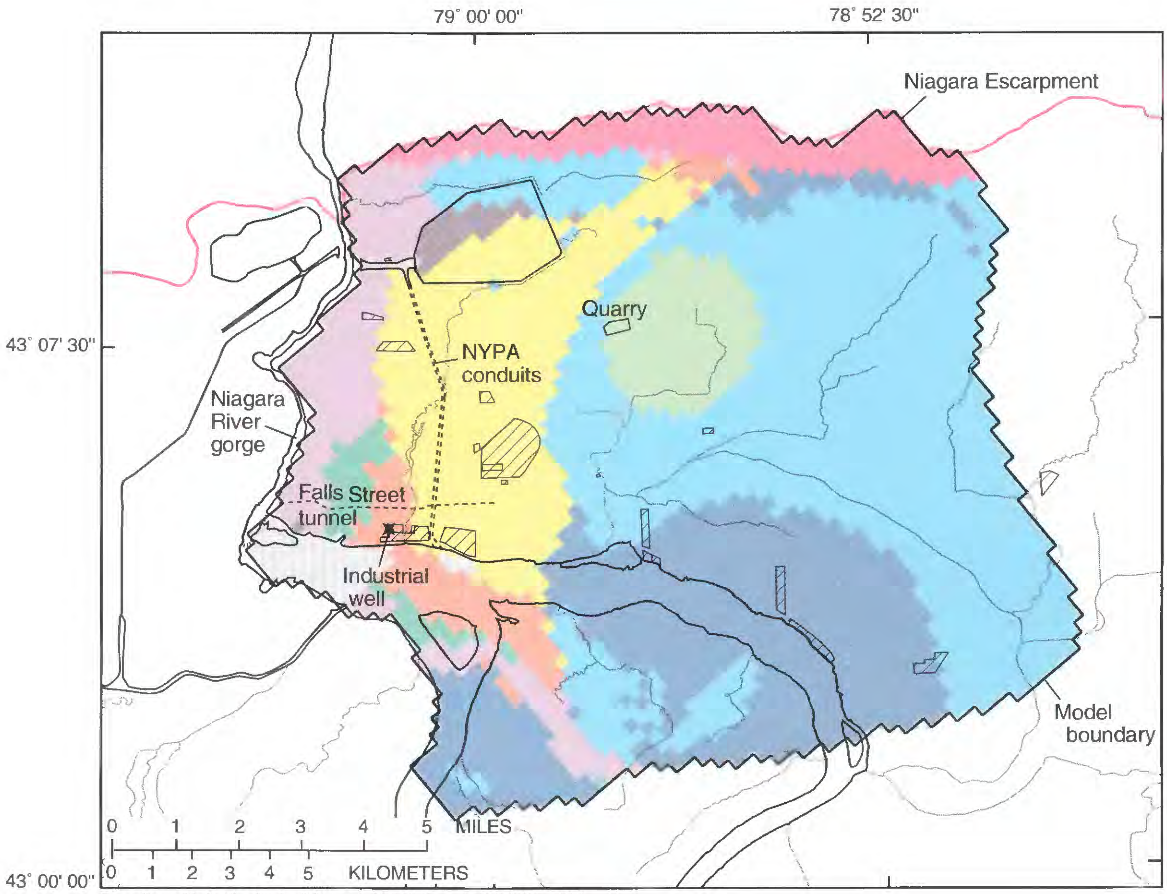

Base from U. S. Geological Survey digital data, 1:100,000, 1983
Universal Transverse Mercator projection, Zone 17

EXPLANATION

Contributing area to point of ground-water discharge:

- Niagara River
- Niagara River gorge
- Perennial streams
- Niagara Escarpment
- Falls Street tunnel at intersection with conduit drain
- Remainder of Falls Street tunnel
- Excavations and springs
- Industrial well
- Forebay canal
- Constant-head or no-flow boundary
- Waste-disposal site

Figure 11A. Contributing areas of discharge boundaries in the weathered bedrock, as computed by the calibrated model.

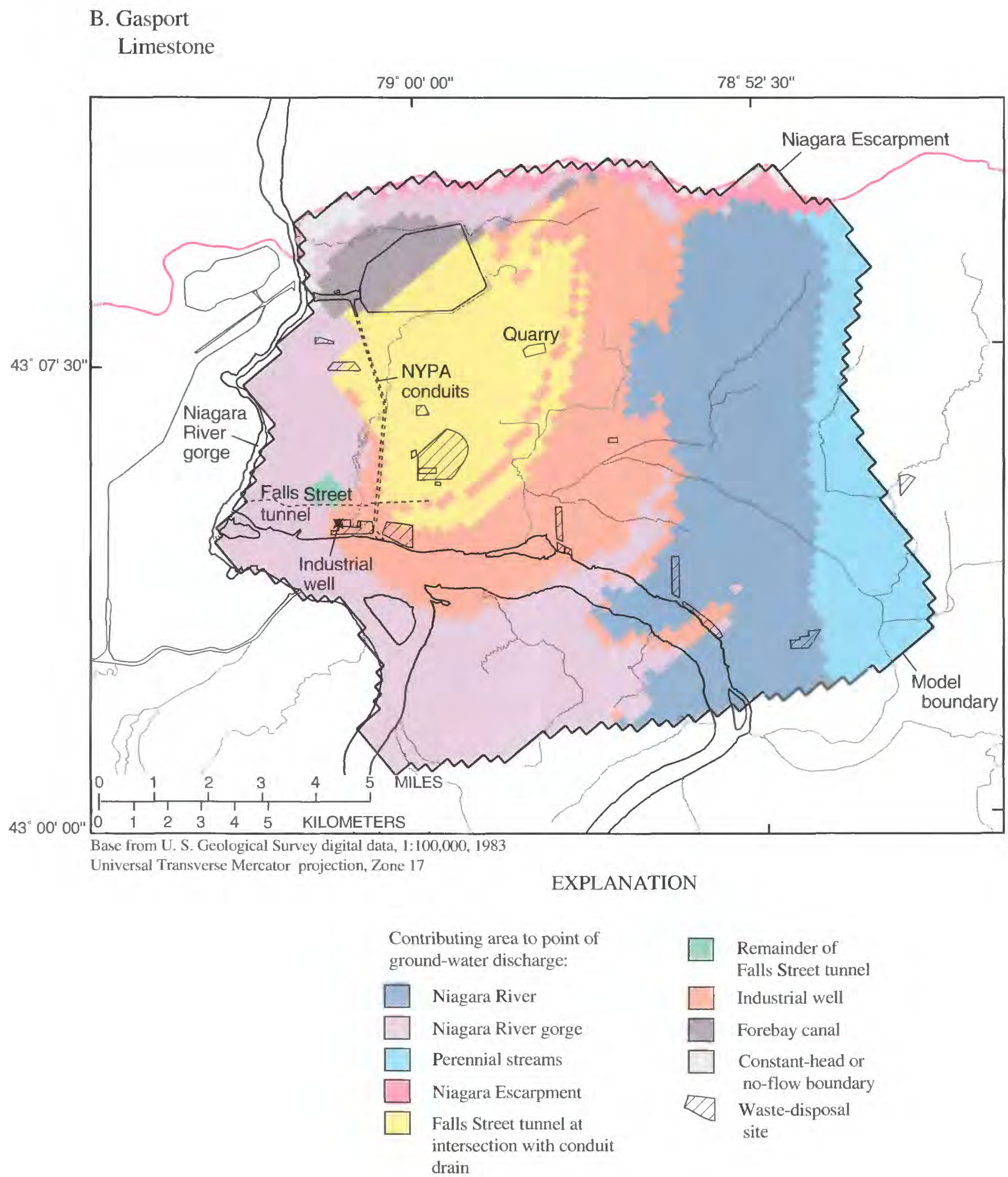

Figure 11B. Contributing areas of discharge boundaries in the Gasport Limestone, as computed by the calibrated model.

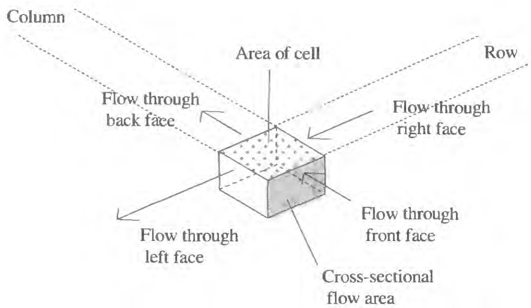

A. Horizontal flow rates through a model cell.

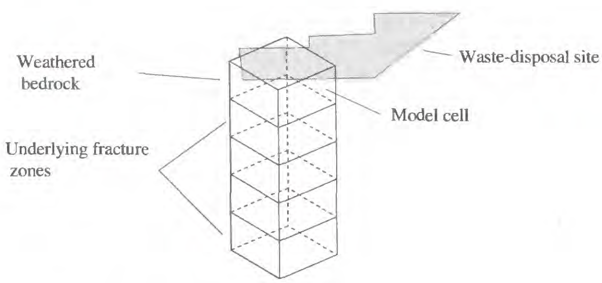

B. Column of model cells used to compute horizontal and vertical Darcy velocity.

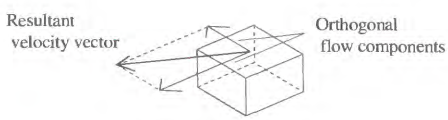

C. Orthogonal flow components and resultant velocity vector.

Figure 12. Calculation of Darcy velocity from flow rates through model cells:

(A) Horizontal flow through a model cell.

(B) Column of model cells used to compute horizontal and vertical Darcy velocity.

(C) Orthogonal flow components and resultant velocity vector.

from the bottom model layer beneath the Niagara River and its tributaries and in areas near the Falls Street tunnel and along the NYPA conduits. Vertical Darcy velocities in the bottom model layer are generally smaller than in the weathered bedrock, although rates also range from less than 10^{-5} to 10^{-2} ft/d. The highest flow rates are upward along the NYPA conduits.

Darcy Velocity Near Selected Waste-Disposal Sites

Horizontal Darcy velocities in the weathered bedrock computed with the calibrated model ranged from 1 to 10^{-3} ft/d and had a mean value of 0.15 ft/d (table 9). The highest velocities were near sites 10 and 12 (fig. 15A, top), which lie along flow paths from the Niagara River to the NYPA conduits. The lowest velocity was near site 21 (table 9 and fig. 15A, bottom), in the southeastern part of the model area, which receives little recharge and where the hydraulic gradient is low.

Horizontal Darcy velocities in the underlying fracture zones were generally an order of magnitude less than those through the weathered bedrock and had a mean value of 0.042 ft/d. The highest velocities were near sites 1 and 6 (fig. 15B, top) within areas of ground-water discharge to the forebay canal and a production well, respectively. The lowest velocity was near site 21 (fig. 15B, bottom).

Vertical Darcy velocities in the weathered bedrock were much less than the horizontal velocities and ranged from 10^{-3} to 10^{-5} ft/d; the mean was 2.8×10^{-4} ft/d. Vertical velocities were highest in the city of Niagara Falls near sites 2, 3, and 6, where the recharge rate is higher than in other parts of the modeled area. The lowest vertical velocity was at site 21.

The directions of horizontal and vertical flow in the weathered bedrock and horizontal flow through underlying fracture zones at each site are indicated in figures 15A and 15B, respectively. Within the city of Niagara Falls, horizontal flow is mainly toward the NYPA conduits or the Niagara River Gorge, and vertical flow is downward from the weathered bedrock to the underlying fracture zones. In the southeastern part of the modeled area, horizontal flow is toward the Niagara River, and vertical flow is generally upward from the underlying fracture zones to the weathered bedrock. Flow directions in the underlying fracture zones generally parallel the directions in the weathered bedrock except near the southern end of the NYPA conduits, where flow is toward the production well at the Buffalo Avenue industrial plant.

Darcy velocities computed by model A are nearly identical to those computed by the calibrated model but differ from those computed by model C. Horizontal Darcy velocities in the weathered bedrock computed by model C are generally greater than those computed by the calibrated model because model C used a much

Table 9. Darcy velocities near selected waste-disposal sites computed with the calibrated model and alternative models A and C

[All values are in feet per day]

		Horizontal Darcy velocity						Vertical Darcy velocity between weathered bedrock and underlying fracture zones[2]		
		Weathered bedrock			Underlying fracture zones					
Number	Site name[1]	Calibrated model	Model A	Model C	Calibrated model	Model A	Model C	Calibrated model	Model A	Model C
1.	Stauffer Chemical	0.15	0.10	0.22	0.17	0.21	0.13	0.00013	0.00016	0.00033
2.	Occidental Hyde Park	.25	.18	.047	.091	.096	.11	.0011	.0013	.00061
3.	SKW Alloys	.12	.095	.20	.039	.045	.0046	.0013	.0015	.00049
4.	Forest Glen	.080	.057	.39	.048	.061	.036	.00008	.00009	.00004
5.	Reichold-Varcum	.088	.060	.43	.045	.055	.036	.00023	.00021	.00012
6.	Olin Buffalo Avenue	.19	.13	.60	.18	.20	.23	.0017	.0016	.00088
7.	Solvent Chemical	.15	.10	.48	.049	.058	.076	.00042	.00046	.00024
8.	Dupont Necco Park	.10	.070	.51	.044	.054	.037	.00029	.00028	.00017
9.	Cecos International	.066	.048	.36	.039	.049	.033	.00033	.00038	.00017
10.	Dupont Buffalo Avenue	1.2	1.2	.91	.034	.041	.054	.00066	.00069	.00063
11.	Great Lakes Carbon	.070	.055	.35	.027	.034	.023	.00014	.00011	.00008
12.	Occidental Buffalo Avenue	.46	.43	.067	.042	.050	.041	.00004	.00004	.00069
13.	Charles Gibson	.0071	.0075	.072	.014	.021	.014	-.00011	-.00013	-.00005
14.	Bell Aerospace	.036	.028	.18	.019	.026	.017	-.00012	-.00010	-.00003
15.	Occidental Love Canal	.017	.013	.075	.0097	.014	.0089	-.00010	-.00013	-.00009
16.	Occidental 102nd Street	.026	.011	.11	.0083	.011	.0073	-.00006	-.00006	-.00004
17.	Olin 102nd Street	.022	.011	.11	.0084	.011	.0073	-.00003	-.00005	-.00003
18.	Niagara County Refuse	.018	.013	.082	.0054	.0064	.0044	-.00001	-.00004	-.00003
19.	Gratwick Riverside Park	.024	.0030	.073	.0013	.00045	.00064	-.00006	-.00002	-.00002
20.	Frontier Chemical	.010	.0078	.0064	.0038	.0055	.0032	-.00005	-.00007	-.00007
21.	Occidental Durez	.0043	.0048	.023	.00026	.00044	.00024	.00001	-.00002	.00001
	Maximum	1.2	1.2	.91	.18	.21	.23	.0017	.0016	.00088
	Minimum (absolute value)	.0043	.0030	.0064	.00026	.00044	.00024	.00001	.00002	.00001
	Mean	.15	.12	.25	.042	.050	.042	.00028	.00030	.00019

[1] Use of firm names is for descriptive purposes only and does not imply endorsement by the U.S. Government.
[2] Positive values indicate downward flow. Negative values indicate upward flow.

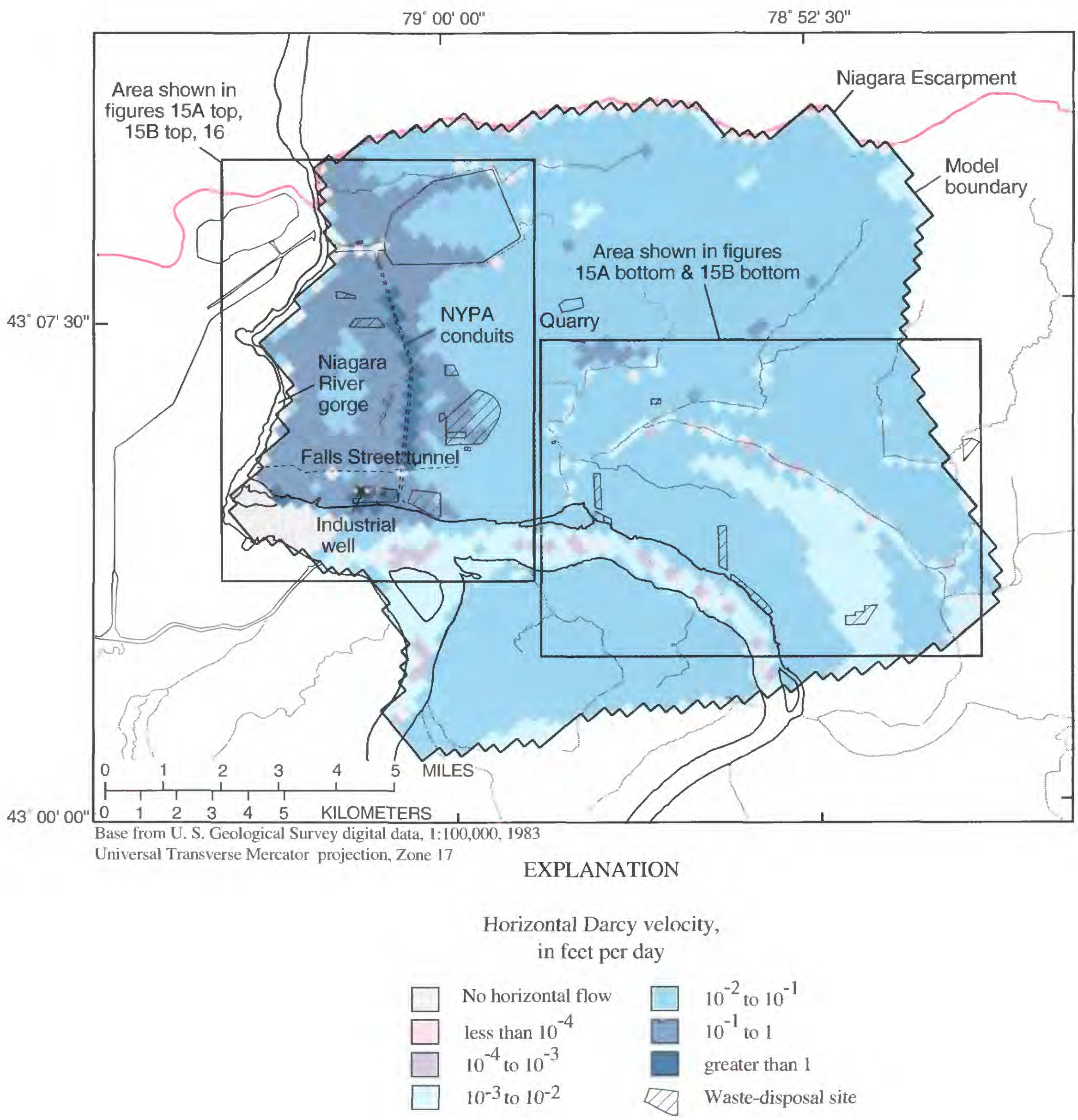

Figure 13A. Horizontal Darcy velocity in the weathered bedrock, as computed with the calibrated model.

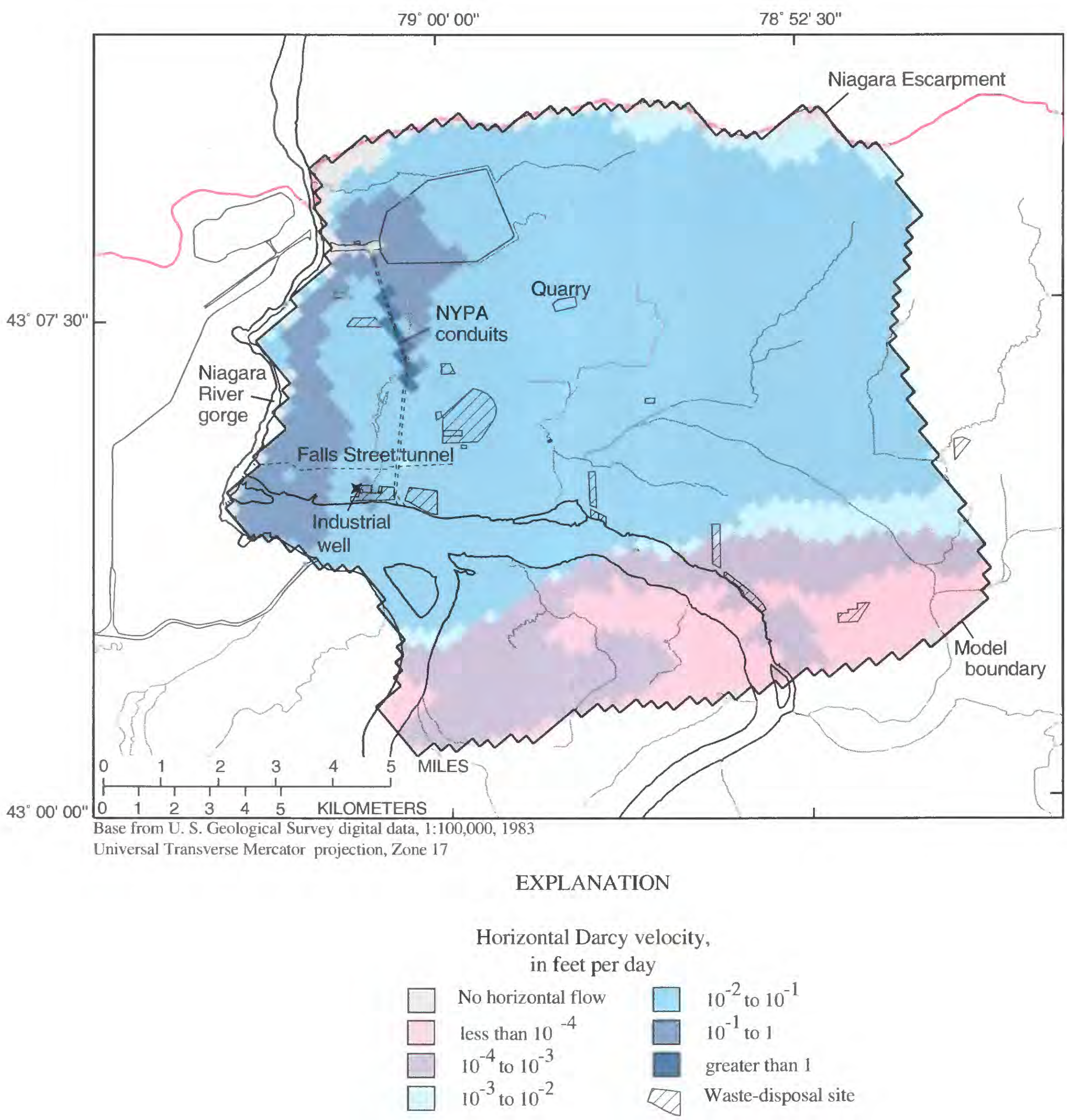

Figure 13B. Horizontal Darcy velocity in the Gasport Limestone, as computed by the calibrated model.

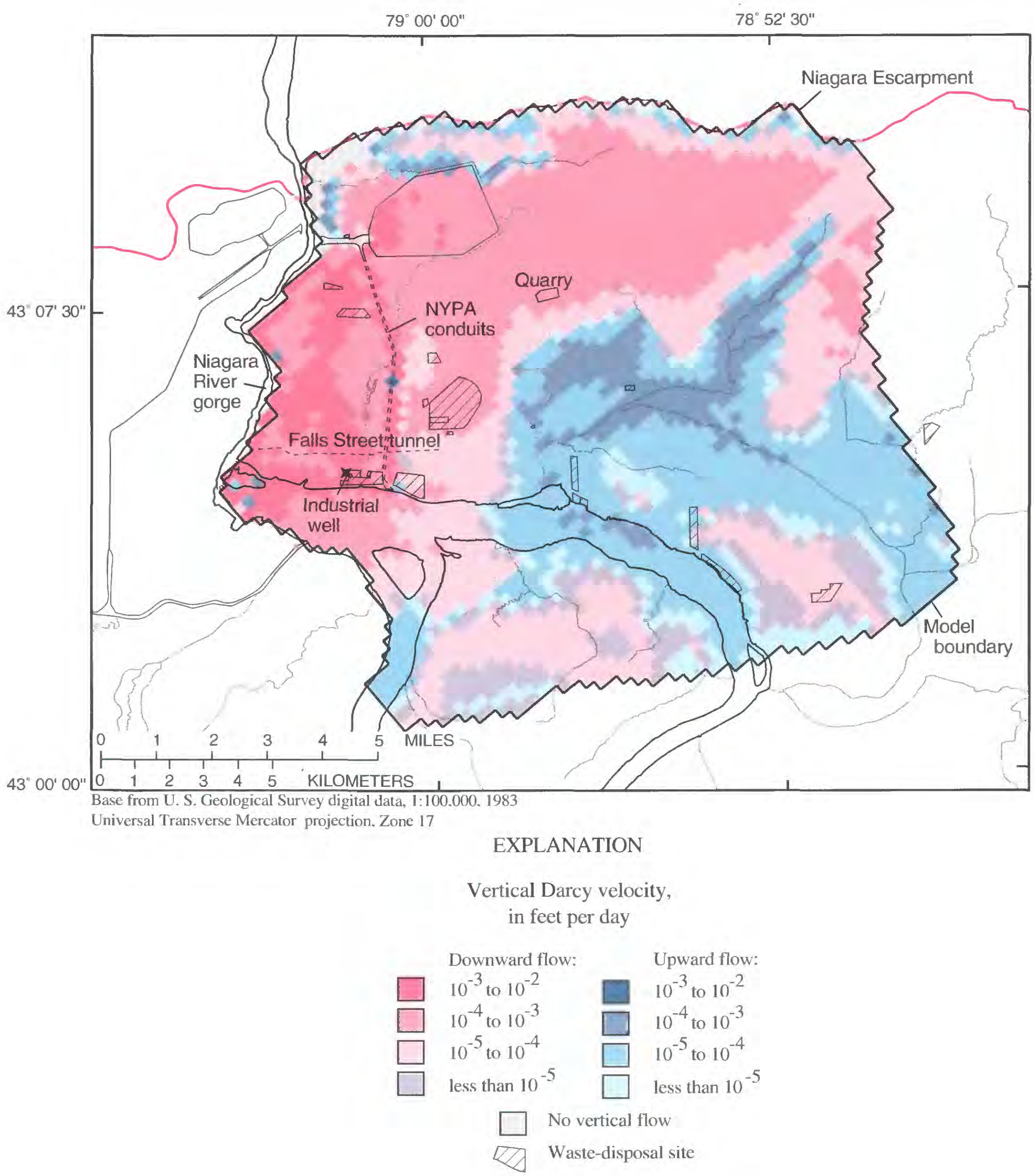

Figure 14A. Vertical Darcy velocity in the weathered bedrock, as computed with the calibrated model.

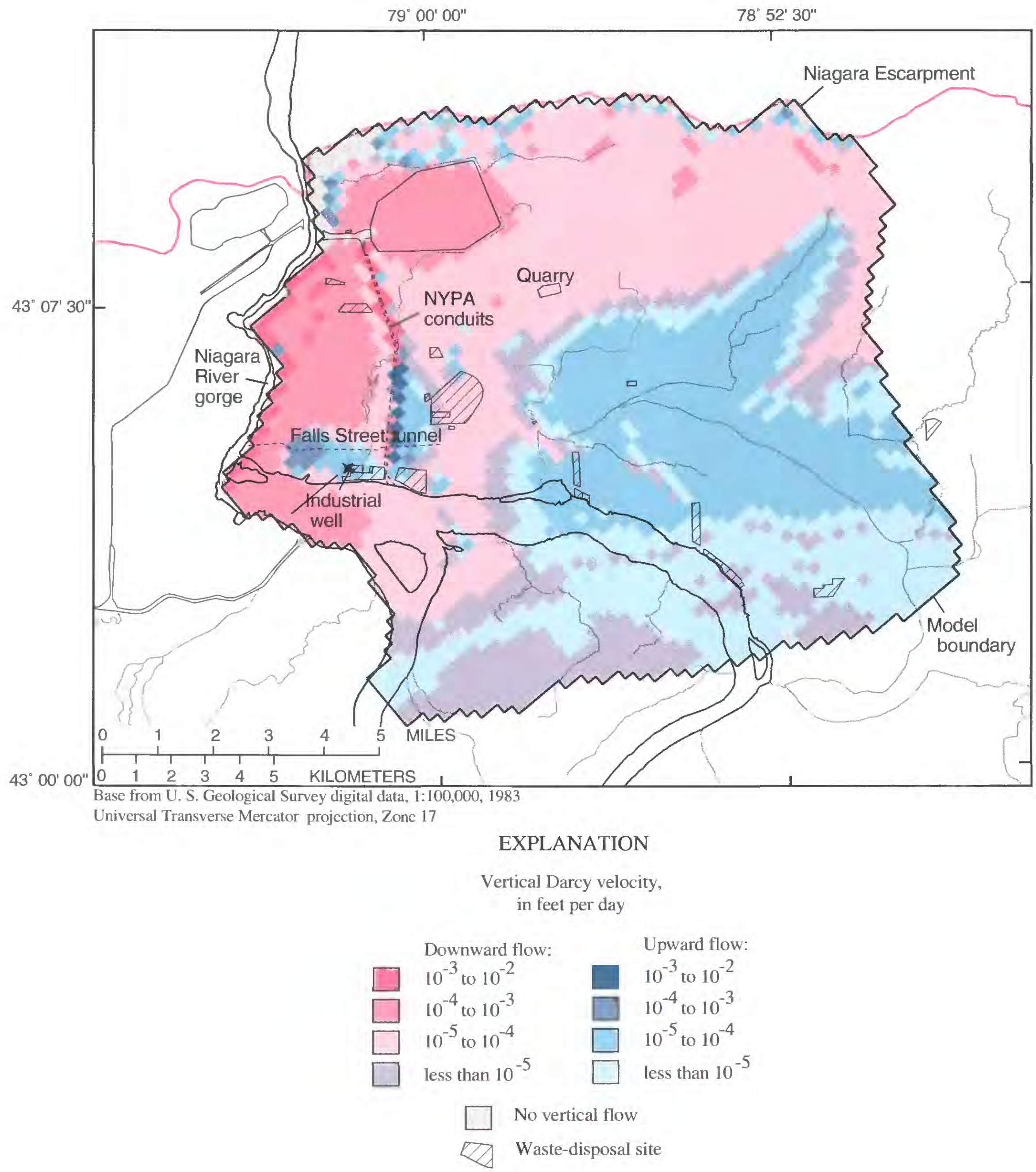

Figure 14B. Vertical Darcy velocity in the Gasport Limestone, as computed with the calibrated model.

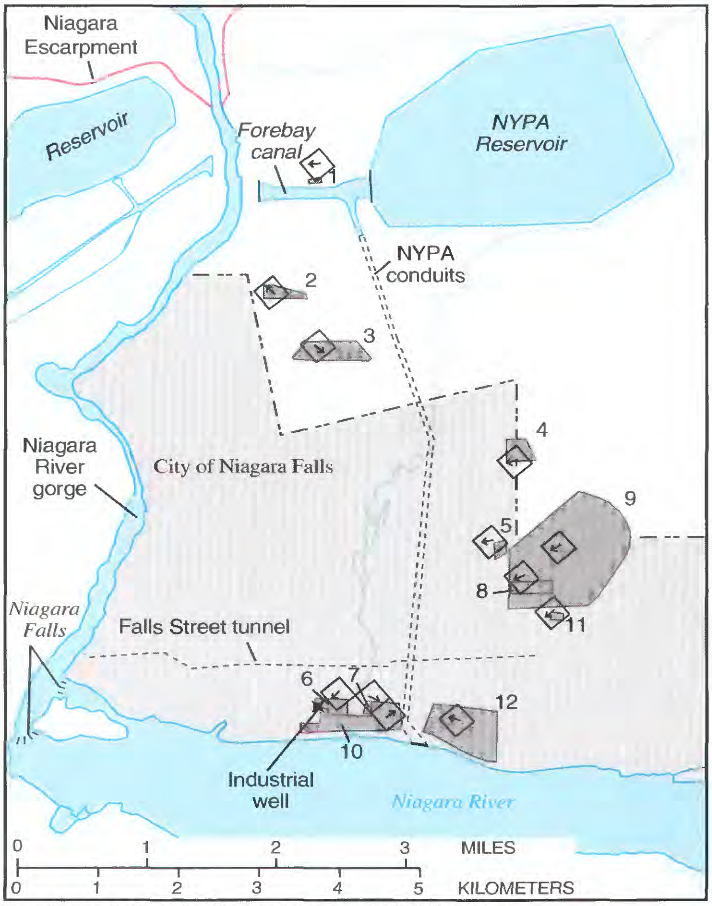

Base from U. S. Geological Survey digital data, 1:100,000, 1983
Universal Transverse Mercator projection, Zone 17

EXPLANATION

21 WASTE-DISPOSAL SITE. Numbers refer to site name in table 9.

MODEL CELL USED TO COMPUTE DARCY VELOCITY. Arrow shows direction of horizontal flow. Dashed line indicates upward vertical flow, otherwise vertical flow is downward.

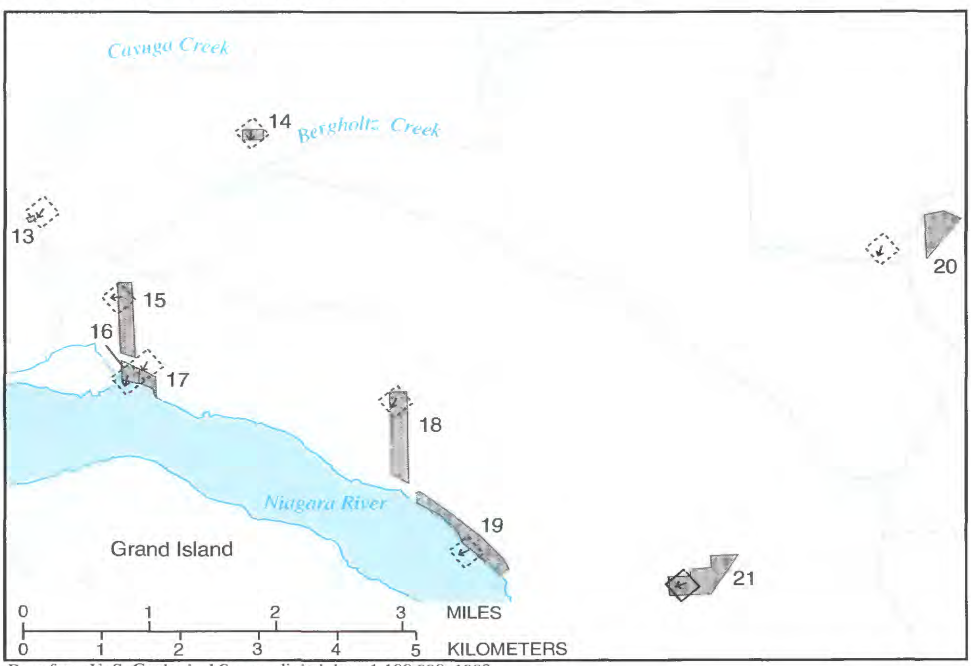

Base from U. S. Geological Survey digital data, 1:100,000, 1983
Universal Transverse Mercator projection, Zone 17

Figure 15A. Directions of horizontal and vertical ground-water flow through weathered bedrock near selected waste-disposal sites in City of Niagara Falls (top), and southeastern part of modeled area (bottom).

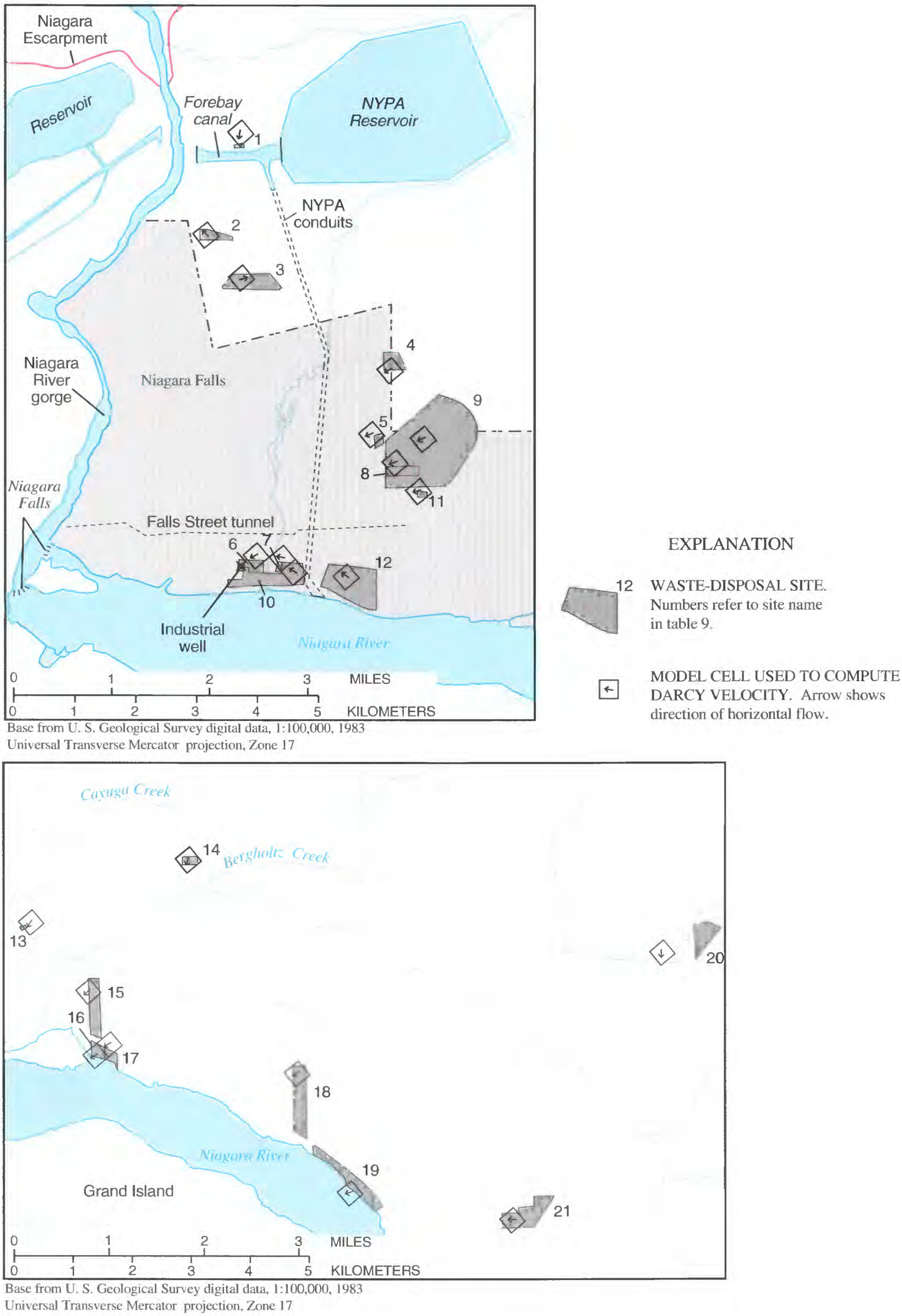

Figure 15B. Directions of horizontal and vertical ground-water flow through underlying fracture zones near selected waste-disposal sites in City of Niagara Falls (top), and southeastern part of modeled area (bottom).

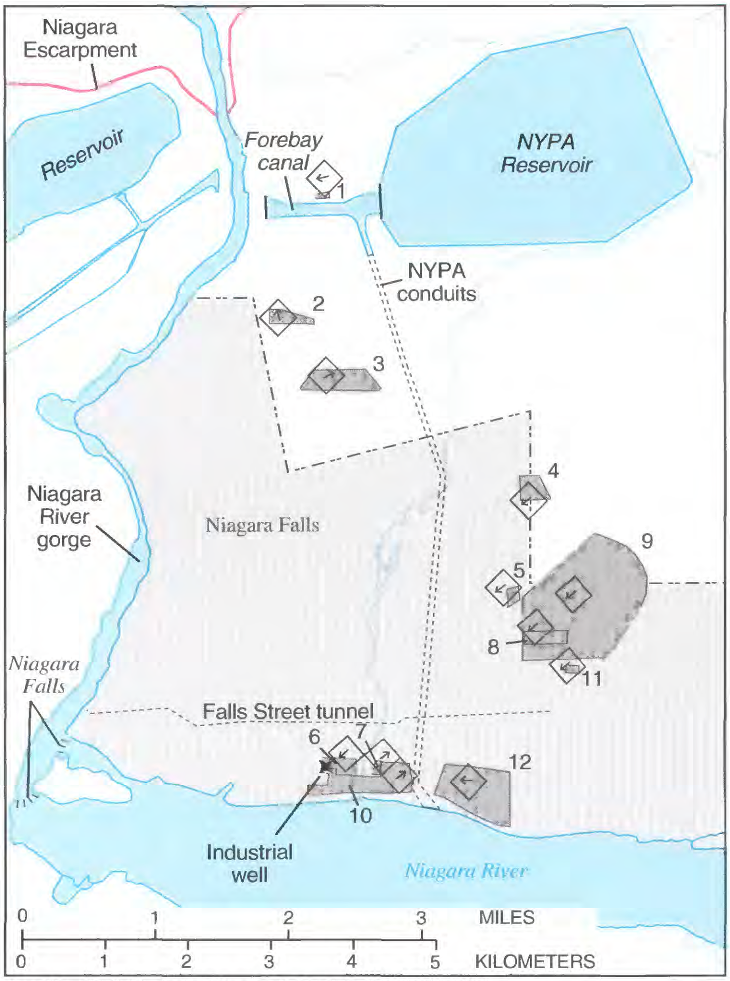

Base from U. S. Geological Survey digital data, 1:100,000, 1983
Universal Transverse Mercator projection, Zone 17

EXPLANATION

12 WASTE-DISPOSAL SITE. Number references site name in table 9.

MODEL CELL USED TO COMPUTE DARCY VELOCITY. Arrow shows direction of horizontal flow. Vertical flow is downward.

Figure 16. Direction of ground-water flow near selected waste-disposal sites in the City of Niagara Falls, based on a horizontal anisotropy of 20:1 in the weathered bedrock (model C).

greater value of transmissivity. Horizontal Darcy velocities at sites 2 and 12 in model C are less than those computed by the calibrated model, however, because the hydraulic gradient in these areas is parallel to the direction of the minimum transmissivity specified in model C (fig. 16). The range in vertical Darcy velocities (10^{-4} to 10^{-5} ft/d) in model C is less than the range computed by the calibrated model because the highest vertical velocities in model C are lower than those computed by the calibrated model.

SUMMARY AND CONCLUSIONS

The Lockport Group consists of 170 ft of virtually undeformed dolomites and limestones of the Lockport Group of the Niagaran Series (Middle Silurian) that strike approximately east-west and dip southward at about 25 ft/mi. Ground water flows primarily through fractures and vugs that have been widened by chemical dissolution in areas where water with a low dissolved-solids concentration circulates through the bedrock. The principal water-bearing zones in the Lockport Group are the weathered bedrock surface and underlying horizontal-fracture zones near stratigraphic contacts. The horizontal-fracture zones are connected by high-angle fractures and by subcrop areas where the fractures intersect the bedrock surface.

The thickness of the weathered bedrock ranges from 10 to 25 ft, and the hydraulic conductivity estimated from aquifer tests ranges from 1 to 200 ft/d. Nine regional horizontal-fracture zones have been delineated through correlation of core logging, outcrop mapping, and hydraulic tests. The transmissivity of the underlying fracture zones, estimated from slug tests, ranges from 30 to 700 ft^2/d. The anisotropy (ratio of horizontal to vertical hydraulic conductivity) of the Lockport Group is estimated to be greater than

70:1 from cross-hole tests in which adjacent fracture zones were isolated with inflatable packers.

Ground water flows through the Lockport Group from topographic highs near the Niagara Escarpment northward toward the escarpment, and southward and westward toward low-lying areas near the Niagara River and outcrop areas along the Niagara River Gorge. Recharge from overlying glacial sediments enters the weathered bedrock and the subcrop areas of the horizontal-fracture zones. Recharge also enters the Lockport Group through infiltration from the Niagara River in areas where the bedrock crops out in the river bottom. Recharge from manmade structures includes infiltration from the Niagara River induced by pumping from an industrial production well along Buffalo Avenue, infiltration from the NYPA reservoir, and leakage from the municipal water supply and unlined storm sewers in the city of Niagara Falls. Ground water discharges to the Niagara River and its tributaries, the Niagara Escarpment, and Niagara River Gorge. Ground water also discharges to the Falls Street tunnel (an unlined storm sewer), primarily where it crosses a drain system surrounding the NYPA conduits.

Ground-water flow through the Lockport Group was simulated with a three-dimensional, finite-difference model in which model layers correspond to horizontal-fracture zones, and vertical leakage represents flow through high-angle fractures. Because the local variation in transmissivity within a fracture zone was assumed to be small in relation to the model-grid spacing, the fracture network within each horizontal-fracture zone was represented as a virtually isotropic, homogeneous porous medium. The model consists of 10 layers that represent: the glacial sediments that overlie the bedrock, the weathered bedrock, and the nine regional water-bearing zones within the Lockport Group. The Salina Shale, which overlies the Lockport Group in the southern part of the modeled area, was also represented.

Lateral boundaries of the modeled area were chosen to correspond to natural hydrologic boundaries, including the Niagara Escarpment and the Niagara River Gorge. Where natural hydrologic boundaries were absent, no-flow or constant-head boundaries were placed in accordance with potentiometric-surface maps of each model layer. Several manmade structures—including the NYPA hydropower-project facilities (intakes, conduits, forebay canal, and reservoir), industrial wells, and tunnels and airshafts excavated in the bedrock within the city of Niagara Falls—were also represented as boundaries within the modeled area.

The model was calibrated to average, steady-state conditions because well hydrographs showed no long-term trends in water levels. Results of the model simulations were compared with (1) 144 measurements of hydraulic head in weathered-bedrock wells, (2) 64 pressure measurements in the horizontal-fracture zones from 13 multilevel piezometers, (3) low-flow measurements of a spring and two streams, and (4) 2 discharge measurements along the Falls Street tunnel and 1 near the Niagara Falls quarry. Parameter values representing hydraulic properties of the aquifer and model boundaries were adjusted during model calibration through a nonlinear-regression method. A set of 15 parameter values were used to represent the aquifer system, 7 of which were estimated through calibration. The estimated parameters included the transmissivity of the weathered bedrock and underlying horizontal-fracture zones; the vertical hydraulic conductivity of the glacial sediments and of the weathered and unweathered bedrock; and the average recharge rate in urban and rural areas.

The hydraulic-head distribution computed by the calibrated model is similar to that contoured from observed data, and the standard error between computed and observed heads is about 10 ft. The maximum error was 30 ft where heads were underestimated near the Niagara Escarpment and overestimated near the NYPA reservoir. Computed discharges were within 60 percent of the observed discharges except at the intersection of the Falls Street tunnel with the NYPA conduits, where the predicted discharge was less than half the observed flow of 930,000 ft^3/d (7.0 Mgal/d), despite the fact that about one quarter of the ground-water flow from the entire modeled area was draining to the tunnel. This discrepancy suggests that an additional source of water not represented in the model is contributing most of the observed flow.

Three alternative models with boundary conditions or parameter distributions that differ from those of the calibrated model were developed to determine whether the aquifer system could be represented by other, equally plausible model designs. Optimum parameter values for three alternative models were obtained through nonlinear regression. One model, in which the conductance of a drain boundary representing the Niagara River Gorge was decreased by a factor of 1,000, was disregarded because the predicted direction of flow in the City of Niagara Falls did not match that indicated by the observed hydraulic gradient. The other two models were judged to be as plausible as the calibrated model. In one model, recharge in the rural zone was divided into upland areas and lowland areas, and the mean recharge rate of the lowland area was estimated to be negative, indicating that ground water discharges upward from the weathered bedrock toward land surface in this area. Results of the other model suggest that horizontal anisotropy in the weathered bedrock could be significant, but the estimated value was uncertain because of correlation between the transmissivity of the weathered bedrock and the recharge rate in the urban area. The optimal values of most of the parameters in the alternative models were within the 95-percent confidence intervals of values estimated with the calibrated model and did not differ by more than 50 percent from the calibrated values. The exception was in the model incorporating horizontal anisotropy, in which the maximum transmissivity of the weathered bedrock was seven times greater than the calibrated value.

The model described in this report is based on the assumption that fracture zones within the Lockport Group can be treated as porous media at the scale of the 1,000-ft cells used in the model. Conclusions concerning ground-water flow rates and direction of flow at a regional scale of several miles are consistent with this assumption. The model might not accurately predict flow paths or advective transport from particular locations within the modeled area, however, because local transmissivity variations not accounted for in the model can greatly affect the rate and direction of ground-water flow.

Results of model simulations indicate that the Falls Street tunnel is a principal discharge point in the modeled area and that many waste-disposal sites are within areas that contribute flow to the tunnel. The recharge rate estimated for urban areas in the city of Niagara Falls is much higher than the rate estimated for rural areas. The source of this additional recharge is unknown but could be conveyance losses in the municipal water supply or infiltration of stormwater from brick-lined sewers that intersect the bedrock. Simulation results also suggest that ground water discharges to land surface in low-lying areas near the Niagara River, but data are insufficient to confirm that discharge in these areas actually occurs.

Results of the simulations indicate that the Niagara River is the likely source of most of the water entering the Falls Street tunnel through an unknown path not represented in the model. An additional model with a smaller geographical extent and decreased cell size could be developed to investigate ground-water flow between the Niagara River, manmade structures, and the Lockport Group near the city of Niagara Falls, which contains several waste-disposal sites. Such a model would represent the hydraulic-head distribution near model boundaries, such as the Niagara River Gorge, in finer detail than the calibrated model discussed here because the cell size would be small enough to reproduce the steep hydraulic gradient in these areas. The smaller model could also be used to investigate alternative explanations for the sources of water entering the Falls Street tunnel and to refine the estimate of the rate of recharge in the city of Niagara Falls, but would require additional investigations to delineate areas of nonuniformity within the fracture zones and to determine their hydraulic properties to enable detailed prediction of flow rates and directions more accurately than the model described in this report.

The parameter-estimation procedure that was used to develop the regional model of the Lockport Group greatly reduced the effort required for model calibration. The complexity of parameter interaction in the 10-layer model would have made calibration by conventional trial-and-error procedures extremely difficult. As many as 10 simulations were completed in a single application of the nonlinear regression, and each decreased the model error. As a result, many more hypotheses about the aquifer system were compared during the course of model calibration than could have been tested through trial-and-error procedures, and better estimates of parameter values were obtained. The nonlinear regression computed the model's sensitivity to each parameter and thereby facilitated (1) identification of parameters to which the model was insensitive, and (2) selection of parameters to include in the regression.

The Darcy velocity (flow rate per unit area) of ground water near 21 selected waste-disposal sites was estimated from results of the calibrated model and two alternative models. The horizontal velocity in the weathered bedrock ranged from 10^{-3} to 1 ft/d, and the velocity through the underlying fracture zones was generally an order of magnitude less. Vertical velocity ranged from 10^{-5} to 10^{-3} ft/d. Velocities estimated by alternative models were similar to those computed by the calibrated model, except for horizontal velocity in the weathered bedrock computed by a model that incorporated horizontal anisotropy (model C). In this model, the maximum transmissivity of the weathered bedrock was greater than in the calibrated model; thus, the horizontal velocities were also greater.

REFERENCES CITED

American Falls International Board, 1974, Presentation and enhancement of the American Falls at Niagara, Appendix C—geology and rock mechanics: Niagara Falls, N.Y., Final Report to the International Joint Commission, June 1974, 71 p.

Brett, C.E., and Calkin, P.E., 1987, Niagara Falls and Gorge, New York-Ontario, *in* Roy, D.C., (ed.), Geological Society of America, Northeastern section centennial field guide: v. 5, p. 97–105.

Brett, C.E., Tepper, D.H., Goodman, W.M., LoDuca, S.T., and Eckert, B.T., 1995, Revised stratigraphy and correlations of the Niagaran Provincial series (Medina, Clinton, and Lockport groups) in the type area of western New York: U.S. Geological Survey Bulletin 2086, 66 p.

Buxton, H.T., and Reilly, T.E., 1987, A technique for analysis of ground-water systems at regional and subregional scales applied on Long Island, New York, *in* Subitzky, Seymour (ed.), Selected papers in the hydrologic sciences 1986: U.S. Geological Survey Water-Supply Paper 2310, p. 129–142.

Camp, Dresser and McKee Environmental Engineers, 1982, City of Niagara Falls, report on Falls Street tunnel, visual inspection and infiltration, air and sediment evaluation: Boston, Mass., Camp, Dresser and McKee Environmental Engineers, 88 p.

Conestoga-Rovers and Associates, 1988, Pump test review and proposed remedial design, Reichold Chemicals, Inc., Niagara Falls, New York: Niagara Falls, N.Y., Conestoga-Rover and Associates, 85 p.

_____ 1990, Remedial investigation final report 102nd Street Landfill site, Niagara Falls, New York: Niagara Falls, N.Y., Conestoga-Rover and Associates, 60 p.

Conestoga-Rovers and Associates and Woodward-Clyde Consultants, 1990, Remedial investigation, 102nd Street landfill site, Niagara Falls, New York: Niagara Falls, N.Y., Conestoga-Rovers and Associates, 161 p.

Cooley, R.L., and Naff, R.C., 1990, Regression modeling of ground-water flow: U.S. Geological Survey Techniques of Water-Resources Investigations Report, Book 3, Chapter B4, 232 p.

Desaulniers, D.E., Cherry, J.A., and Fritz, P., 1981, Origin, age and movement of pore water in argillaceous Quarternary deposits at four sites in southwestern Ontario: Journal of Hydrology, v. 50, p. 231–257.

Draper, N.R., and Smith, Harry, 1981, Applied regression analysis (2nd ed.): New York, John Wiley, 709 p.

E.C. Jordan Co., 1985, Love Canal remedial project, Love Canal long-term monitoring program design: Portland, Me., E.C. Jordan Co., 163 p.

Ecology and Environment, 1987, Analysis and interpretation of pumping test performed December 1986 at the Carborundum Specialty Products site, Sanborn, N.Y.: Buffalo, N.Y., Ecology and Environment, 36 p.

Fisher, D.W., and Brett, C.E., 1981, The geologic past, *in* Tesmer, I.H., (ed.), Colossal cataract—the geologic history of Niagara Falls: Albany, N.Y., State University of New York Press, p. 16–42.

Geotrans, Inc., 1987, Necco Park regional ground-water study status report, Niagara Falls, New York: Boxborough, Mass., Geotrans, Inc., 47 p.

Golder and Associates 1987, Results of Phase I and II investigations, Bell Aerospace Textron Wheatfield, New York: Mississauga, Ontario, Canada, Golder and Associates, 35 p.

_____ 1990a, Geotechnical investigation of proposed Empire State pipeline, Tonawanda channel crossing, Niagara River: Mississauga, Ontario, Canada, Golder and Associates, 8 p.

_____ 1990b, Result of the pump-in and pump-out testing, Bell Aerospace Textron, Niagara Falls, New York: Mt. Laurel, N.J., Golder and Associates, 68 p.

Gross, M.C., and Engelder, T., 1991, A case for neotectonic joints along the Niagara Escarpment: Tectonics, v. 10, no. 3, p. 631–641.

Ground Water Associates, 1986, Aquifer test and top-of-rock characterization, Cecos International, Niagara Falls, New York: Westerville, Ohio, Ground Water Associates, 51 p.

Helsel, D.R., and Hirsch, R.M., 1992, Statistical methods in water resources: Amsterdam, The Netherlands, Elsevier, 522 p.

Hill, M.C., 1992, A computer program (MODFLOWP) for estimating parameters of a transient, three-dimensional ground-water flow model using nonlinear regression: U.S. Geological Survey Open-File Report 91–484, 382 p.

Johnston, R.H., 1964, Ground water in the Niagara Falls area, New York: State of New York Water Resources Commission Bulletin GW 53, 93 p.

Kappel, W.M., and Tepper, D.H., 1992, An overview of the recent U.S. Geological Survey study of the hydrogeology of the Niagara Falls area of New York *in* Modern Trends in hydrogeology, 1992 Conference of Canadian National Chapter International Association of Hydrogeologists, Hamilton, Ontario, p. 609–622.

Legette, Brashears, and Graham, Inc., 1979, Progress report 6: Shallow ground-water quality investigation, Hooker Chemicals and Plastics Corporation, Niagara Falls, New York: Wilton, Conn., Legette, Brashears, and Graham, Inc., 13 p.

McDonald, M.G., and Harbaugh, A.W., 1988, A modular three-dimensional finite-difference ground-water flow model: U.S. Geological Survey Techniques of Water-Resources Investigations, Book 6, Chap. A1.

Maslia, M.L., and Johnston, R.H., 1984, Use of a digital model to evaluate hydrogeologic controls on ground-water flow in a fractured rock aquifer at Niagara Falls, New York, USA: Journal of Hydrology, v. 79, p. 167–194.

Mercer, J.W., Silka, L.R., and Faust, C.R., 1983, Modeling ground-water flow at Love Canal, New York: Journal of Environmental Engineering, v. 109, no. 4, p. 924–942.

Miller, T.S., and Kappel, W.M., 1987, Effect of Niagara Power Plant project on ground-water flow in the upper part of the Lockport Dolomite, Niagara Falls area, New York: U.S. Geological Survey Water-Resources Investigations Report 86–4130, 31 p.

New York Power Authority, 1986, Niagara power project expansion report of the chemical contamination field investigation conducted in 1985–1986: New York, N.Y., New York Power Authority, 123 p.

Niagara River Toxics Committee, 1984, Report of the Niagara River Toxics Committee: Environment Canada, Ontario Ministry of the Environment, U.S. Environmental Protection Agency, New York State Department of Environmental Conservation, 356 p.

Noll, R.S., 1986, Geochemistry and hydrology of ground-water flow systems in the Lockport Dolomite near Niagara Falls, New York: Syracuse, N.Y., Syracuse University,Unpublished Master's thesis, 143 p.

Novakowski, K.S., and Lapcevic, P.A., 1988, Regional hydrogeology of the Silurian and Ordovician sedimentary rock underlying Niagara Falls, Ontario, Canada: Journal of Hydrology, v. 104, p. 211–236.

Papadopulos, I.S., 1965, Nonsteady flow to a well in an infinite anisotropic aquifer; *in* Proceedings of the Dubrovnic Symposium on the hydrology of fractured rock: International Association of Scientific Hydrology, p. 21–31.

Pollock, D.W., 1989, Documentation of computer programs to compute and display pathlines using results from the U.S. Geological Survey modular three-dimensional finite-difference ground-water flow model: U.S. Geological Survey Open-File Report 89–381, 188 p.

Scott, J.C., 1990, A statistical processor for analyzing simulations made using the modular finite-difference ground-water flow model: U.S. Geological Survey Water-Resources Investigations Report 89-4159, 218 p.

Stephens, M.A., 1974, EDF statistics for goodness of fit and some comparisons: Journal of the American Statistical Association, no. 69, p. 730–737.

Tepper, D.H., 1989, Techniques for delineation of regional water-bearing zones in the Lockport Dolomite, Niagara Falls area, New York [abs.]; *in* Abstracts with Programs: Geological Society of America, 24th Annual Meeting of the Northeastern Section, v. 21, no. 2, p. 70.

Tepper, D.H., Goodman, W.M., and Brett, C.E., 1991, Stratigraphic and structural controls on the development of regional water-bearing zones in the Lockport Group in the Niagara Falls area, New York [abs.], *in* Abstracts with Programs: Geological Society of America, 26th Annual Meeting, v. 23, no. 5, p. 267.

Woodward-Clyde Consultants, 1983, Geohydrologic investigations, Niagara Plant, Niagara Falls, New York: Plymouth Meeting, Pa., Woodward-Clyde Consultants, 58 p.

_____ 1984, Supplemental site assessment studies, Necco Park, Niagara Falls: Plymouth Meeting, Pa., Woodward-Clyde Consultants, 48 p.

_____ 1988, Evaluation of December 1987 aquifer test results, Necco Park, Niagara Falls, New York: Plymouth Meeting, Pa., Woodward-Clyde Consultants, 20 p.

_____ 1989, Interpretive report for Necco Park and I. duPont de Nemours and Company, Niagara Falls, New York: Plymouth Meeting, Pa., Woodward-Clyde Consultants, 97 p.

Yager, R.M., and Kappel W.M., 1987, Characterization of fractures in the Lockport Dolomite, Niagara County, New York, *in* Khanbilvardi, R.M., and Fillos, J., (eds.), Pollution, risk assessment and remediation in ground-water systems: Washington, D.C., Scientific Publications Co., p. 149–195.

Yager, R.M., and Hill, M.C., 1991, Comparison of hypotheses used to construct simulations of transient three-dimensional ground-water flow by nonlinear regression, [abs.] *in* EOS, 1991: Fall Meeting Abstract Supplement: American Geophysical Union, p. 210.

SELECTED SERIES OF U.S. GEOLOGICAL SURVEY PUBLICATIONS

Periodical

Preliminary Determination of Epicenters (issued monthly).

Technical Books and Reports

Professional Papers are mainly comprehensive scientific reports of wide and lasting interest and importance to professional scientists and engineers. Included are reports on the results of resource studies and of topographic, hydrologic, and geologic investigations. They also include collections of related papers addressing different aspects of a single scientific topic.

Bulletins contain significant data and interpretations that are of lasting scientific interest but are generally more limited in scope or geographic coverage than Professional Papers. They include the results of resource studies and of geologic and topographic investigations, as well as collections of short papers related to a specific topic.

Water-Supply Papers are comprehensive reports that present significant interpretive results of hydrologic investigations of wide interest to professional geologists, hydrologists, and engineers. The series covers investigations in all phases of hydrology, including hydrogeology, availability of water, quality of water, and use of water.

Circulars present administrative information or important scientific information of wide popular interest in a format designed for distribution at no cost to the public. Information is usually of short-term interest.

Water-Resources Investigations Reports are papers of an interpretive nature made available to the public outside the formal USGS publications series. Copies are reproduced on request unlike formal USGS publications, and they are also available for public inspection at depositories indicated in USGS catalogs.

Open-File Reports include unpublished manuscript reports, maps, and other material that are made available for public consultation at depositories. They are a nonpermanent form of publication that may be cited in other publications as sources of information.

Maps

Geologic Quadrangle Maps are multicolor geologic maps on topographic bases in 7.5- or 15-minute quadrangle formats (scales mainly 1:24,000 or 1:62,500) showing bedrock, surficial, or engineering geology. Maps generally include brief texts; some maps include structure and columnar sections only.

Geophysical Investigations Maps are on topographic or planimetric bases at various scales; they show results of surveys using geophysical techniques, such as gravity, magnetic, seismic, or radioactivity, which reflect subsurface structures that are of economic or geologic significance. Many maps include correlations with the geology.

Miscellaneous Investigations Series Maps are on planimetric or topographic bases of regular and irregular areas at various scales; they present a wide variety of format and subject matter. The series also includes 7.5-minute quadrangle photogeologic maps on planimetric bases that show geology as interpreted from aerial photographs. Series also includes maps of Mars and the Moon.

Coal Investigations Maps are geologic maps on topographic or planimetric bases at various scales showing bedrock or surficial geology, stratigraphy, and structural relations in certain coal-resource areas.

Oil and Gas Investigations Charts show stratigraphic information for certain oil and gas fields and other areas having petroleum potential.

Miscellaneous Field Studies Maps are multicolor or black-and-white maps on topographic or planimetric bases for quadrangle or irregular areas at various scales. Pre-1971 maps show bedrock geology in relation to specific mining or mineral-deposit problems; post-1971 maps are primarily black-and-white maps on various subjects such as environmental studies or wilderness mineral investigations.

Hydrologic Investigations Atlases are multicolored or black-and-white maps on topographic or planimetric bases presenting a wide range of geohydrologic data of both regular and irregular areas; principal scale is 1:24,000, and regional studies are at 1:250,000 scale or smaller.

Catalogs

Permanent catalogs, as well as some others, giving comprehensive listings of U.S. Geological Survey publications are available under the conditions indicated below from the U.S. Geological Survey, Information Services, Box 25286, Federal Center, Denver, CO 80225. (See latest Price and Availability List.)

"Publications of the Geological Survey, 1879–1961" may be purchased by mail and over the counter in paperback book form and as a set of microfiche.

"Publications of the Geological Survey, 1962–1970" may be purchased by mail and over the counter in paperback book form and as a set of microfiche.

"Publications of the U.S. Geological Survey, 1971–1981" may be purchased by mail and over the counter in paperback book form (two volumes, publications listing and index) and as a set of microfiche.

Supplements for 1982, 1983, 1984, 1985, 1986, and for subsequent years since the last permanent catalog may be purchased by mail and over the counter in paperback book form.

State catalogs, "List of U.S. Geological Survey Geologic and Water-Supply Reports and Maps For (State)," may be purchased by mail and over the counter in paperback booklet form only.

"Price and Availability List of U.S. Geological Survey Publications," issued annually, is available free of charge in paperback booklet form only.

Selected copies of a monthly catalog "New Publications of the U.S. Geological Survey" are available free of charge by mail or may be obtained over the counter in paperback booklet form only. Those wishing a free subscription to the monthly catalog "New Publications of the U.S. Geological Survey" should write to the U.S. Geological Survey, 582 National Center, Reston, VA 20192.

Note—Prices of Government publications listed in older catalogs, announcements, and publications may be incorrect. Therefore, the prices charged may differ from the prices in catalogs, announcements, and publications.